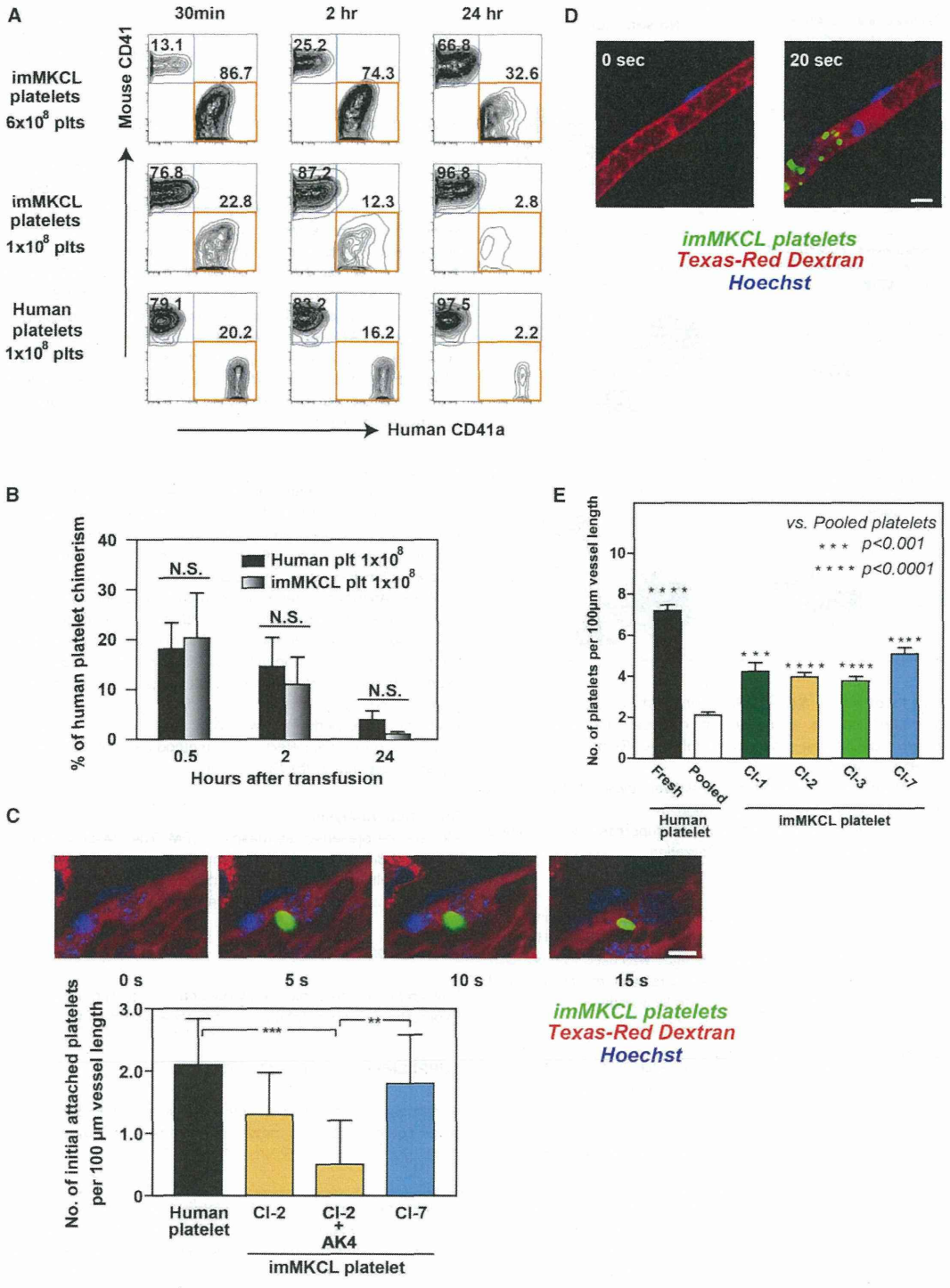

Figure 6. imMKCL-Derived Platelets Show Circulation Potential and Intact In Vivo Functionality in a Thrombocytopenic Mouse Model

(A) Platelet transfusion model in which NOG mice were irradiated (2.4 Gy) in order to induce thrombocytopenia. Nine days later, imMKCL-derived platelets (6×10^8 or 1×10^8) and human PB-derived platelets (1×10^8) were injected via the tail vein. Shown are representative contour plots of samples from a transfused mouse. Detected are mouse $CD41^+$ and human $CD41a^+$ cells 30 min, 2 hr, and 24 hr after transfusion.

(B) Platelet chimerism was quantified by flow cytometry. Circulation of injected platelets was evaluated after 30 min, 2 hr, and 24 hr. N = 4 individual groups from two independent experiments.

(legend continued on next page)

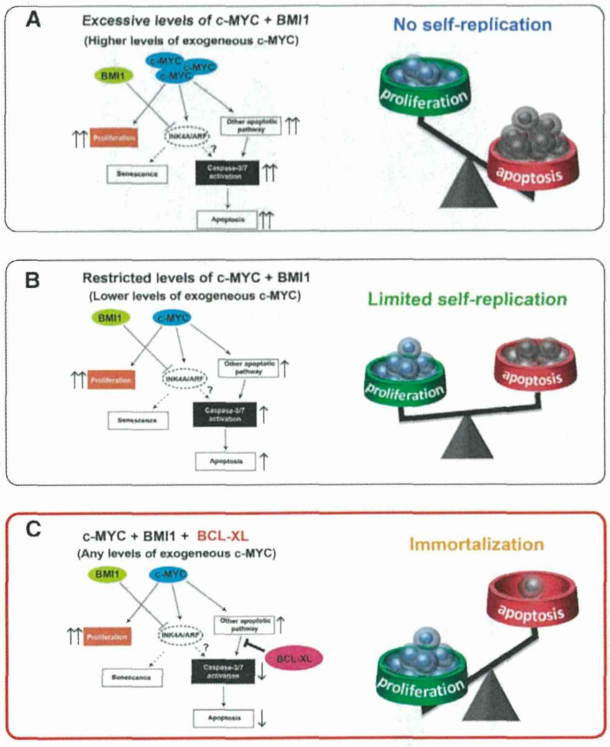

Figure 7. Models of MKCL Self-Replication Systems

(A) Excessive c-MYC induces strong activation of caspase 3 and 7 and apoptotic pathways, despite the suppression of INK4A/ARF by ectopic BMI1, leading to no self-replication.

(B) Appropriate activation of c-MYC induces a relatively low level of caspase 3 and 7 activation, leading to limited self-replication.

(C) Added BCL-XL acts in concert with BMI1 to suppress c-MYC-related apoptotic pathways, leading to MKCL immortalization.

(Eto et al., 2007; Takayama et al., 2010). We amplified the DD-encoding sequence from pPTunerC vector and Shield1 (Clontech and Takara Biotechnology) to generate the *cMYC-DD* construct. Shield1 was used to block DD-domain-mediated protein degradation. The use of viral vectors was approved by committees at the University of Tokyo or Kyoto University.

Cell Culture

On day 14 of culture, during hematopoietic differentiation from hESCs and hiPSCs (Takayama et al., 2008), HPCs were collected and transferred onto irradiated C3H10T1/2 cells in the presence of 50 ng/ml human SCF (R&D Systems) and 50 ng/ml human TPO (R&D) (Takayama et al., 2010). Gene expression was controlled by the presence or absence of 2 μM β-estradiol or 1 μg/ml doxycycline (Clontech) for modified pMXs inducible vector or the presence of 1 μg/ml doxycycline for Ai-LV, respectively. MK differentiation from CB $CD34^+$ cell was accomplished as described previously (Proulx et al., 2004).

In Vitro Analysis of imMKCLs, imMKCL Platelets, and Human Platelets

qRT-PCR, cell-surface markers of imMKCLs and platelets, electron microscopy, and PAC-1 binding were examined as described previously (Takayama et al., 2010). Flow-cytometry-based platelet aggregation assays were performed as described previously (De Cuyper et al., 2013). Clot retraction assays were carried out as described previously (Takizawa et al., 2010). An ex vivo flow chamber precoated with human vWF (10 μg/ml, provided by K. Soejima, Kaketsuken) was utilized to observe shear (1,600 s^{-1})-dependent thrombus formation under an inverted microscope equipped with fluorescence (Nikon A1R) and microfluid systems (Ibidi Products). Platelets were stained with CFSE dye (5 μM, Invitrogen) and used in the presence of CD42b (HIP1; Abcam; 10 μg/ml) or isotype-matched antibodies (BioLegend). Human pooled platelets were prepared by 5-day culture at 37°C under serum-free conditions.

In Vivo Analysis in Mice

Nine days later, irradiation in NOG mice, fresh or pooled human platelets from a donor, or imMKCL-derived platelets were intravenously administered (100 μl). Then, blood samples (50–100 μl) were collected from the retro-orbital plexus in the mice 30 min, 2 hr, and 24 hr after transfusion. The samples were labeled with human CD41a-APC and mouse CD41-PE antibodies (EMFRET Analytics), after which chimerism was analyzed. Similar NOG mice with thrombocytopenia were also used for in vivo imaging studies. To visually analyze thrombus formation in the microcirculation of the mesentery in living animals, we used in vivo laser- and reactive-oxygen-species-induced injury with a visualization technique developed through modification of conventional methods (Nishimura et al., 2012; Takizawa et al., 2010). Some experiments were performed with AK4 (human P-selectin antibody; Abcam; 20 μg/ml). Additional details of the methods and other information for imaging are presented in the Supplemental Information.

Statistical Analysis

All data are presented as means ± SEM. The statistical significance of the observed differences was determined with one-way ANOVA followed by Tukey's multiple comparison test and two-tailed Student's t tests for pairwise comparisons. Values of $p < 0.05$ were considered significant.

ACCESSION NUMBERS

Raw and normalized microarray data have been deposited in the NCBI Gene Expression Omnibus database under accession number GSE54168.

SUPPLEMENTAL INFORMATION

Supplemental Information contains Supplemental Experimental Procedures, seven figures, and three movies and can be found with this article online at http://dx.doi.org/10.1016/j.stem.2014.01.011.

(C) Time-lapse confocal microscopy showing potential in vivo platelet function. Mice were transfused with 1 × 10^8 platelets derived from different groups. Top: representative sequential images showing initial adhesion by imMKCL-derived platelets onto injured vessel walls. CSFE-labeled imMKCL platelets (Cl-2 and Cl-7; green) along with dextran (Texas Red) are shown. Bottom: the number of initially attached platelets per 100 μm vessel length were counted. Actual results are shown in Movie S2. The results are averaged data from 40 vessels from three to five animals in each group. N.S., not significant; ***$p < 0.001$, ****$p < 0.0001$. AK4; human P-selectin antibody. The scale bar represents 10 μm.

(D) Representative sequential images showing thrombus formation by imMKCL-derived platelets within a small capillary and artery. CSFE-labeled imMKCL platelets (green) along with dextran (Texas Red) are shown. Hematoporphyrin was administrated in order to induce thrombus formation prior to laser-induced injury. Platelets adhered to the site of laser injury, finally contributing to the complete occlusion of vessels. Original videos are available as Movie S3. The scale bars represent 10 μm.

(E) Fresh donor platelets, pooled donor platelets, and imMKCL-derived platelets incorporated into thrombi were quantified. Pooled platelets were stored for 5 days at 37°C. Platelets from imMKCL Cl-1, Cl-2, Cl-3, and Cl-7 were used. The results summarize four independent experiments (n = 40 vessels from three to five animals for each group). N.S., not significant; ***$p < 0.001$, ****$p < 0.0001$.

ACKNOWLEDGMENTS

The authors thank H. Suemori, T. Kitamura, M. Onodera, H. Mano, M. Nakanishi, R. Mulligan, H. Kashiwagi, K. Soejima, and Y. Kurose. Electron microscopy was supported by Integrated Imaging Research Support (nonprofit organization). This work was supported by grants-in-aid from MEXT (K.E.) and the Project of Realization of Regenerative Medicine and Highway Program from MEXT/JST (K.E.), A-STEP, and CREST from JST (K.E.) and a Health Labor Sciences Research Grant from the Ministry of Health Labor and Welfare (K.E.). This research was also supported in part by the first Program from JSPS (S.Y.). Visiting fellows S.H. (Kaken Pharmaceutical), T.K. (Nissan Chemical), and K.H. (Toray Industries) were supported by each company. S.Y. is a member without salary of scientific advisory board (SAB) of iPierian, iPS Academia Japan, Megakaryon, and HEALIOS K. K. Japan. H.N. and K.E. are members without salary of SAB of Megakaryon. H.N. is an outside board member of ReproCELL. S.N., N.T., H.N., and K.E. submitted the patent related with this manuscript.

Received: January 31, 2013
Revised: October 2, 2013
Accepted: January 12, 2014
Published: February 13, 2014

REFERENCES

Banaszynski, L.A., Chen, L.C., Maynard-Smith, L.A., Ooi, A.G., and Wandless, T.J. (2006). A rapid, reversible, and tunable method to regulate protein function in living cells using synthetic small molecules. Cell *126*, 995–1004.

Bergmeier, W., Burger, P.C., Piffath, C.L., Hoffmeister, K.M., Hartwig, J.H., Nieswandt, B., and Wagner, D.D. (2003). Metalloproteinase inhibitors improve the recovery and hemostatic function of in vitro-aged or -injured mouse platelets. Blood *102*, 4229–4235.

Chen, C., Fuhrken, P.G., Huang, L.T., Apostolidis, P., Wang, M., Paredes, C.J., Miller, W.M., and Papoutsakis, E.T. (2007). A systems-biology analysis of isogenic megakaryocytic and granulocytic cultures identifies new molecular components of megakaryocytic apoptosis. BMC Genomics *8*, 384.

De Cuyper, I.M., Meinders, M., van de Vijver, E., de Korte, D., Porcelijn, L., de Haas, M., Eble, J.A., Seeger, K., Rutella, S., Pagliara, D., et al. (2013). A novel flow cytometry-based platelet aggregation assay. Blood *121*, e70–e80.

Eto, K., Nishikii, H., Ogaeri, T., Suetsugu, S., Kamiya, A., Kobayashi, T., Yamazaki, D., Oda, A., Takenawa, T., and Nakauchi, H. (2007). The WAVE2/Abi1 complex differentially regulates megakaryocyte development and spreading: implications for platelet biogenesis and spreading machinery. Blood *110*, 3637–3647.

Fuentes, R., Wang, Y., Hirsch, J., Wang, C., Rauova, L., Worthen, G.S., Kowalska, M.A., and Poncz, M. (2010). Infusion of mature megakaryocytes into mice yields functional platelets. J. Clin. Invest. *120*, 3917–3922.

Gardiner, E.E., Al-Tamimi, M., Andrews, R.K., and Berndt, M.C. (2012). Platelet receptor shedding. Methods Mol. Biol. *788*, 321–339.

Hirata, S., Takayama, N., Jono-Ohnishi, R., Endo, H., Nakamura, S., Dohda, T., Nishi, M., Hamazaki, Y., Ishii, E.I., Kaneko, S., et al. (2013). Congenital amegakaryocytic thrombocytopenia iPS cells exhibit defective MPL-mediated signaling. J. Clin. Invest. *123*, 3802–3814.

Hirose, S., Takayama, N., Nakamura, S., Nagasawa, K., Ochi, K., Hirata, S., Yamazaki, S., Yamaguchi, T., Otsu, M., Sano, S., et al. (2013). Immortalization of erythroblasts by c-MYC and BCL-XL enables large-scale erythrocyte production from human pluripotent stem cells. Stem Cell Reports *1*, 499–508.

Hotti, A., Järvinen, K., Siivola, P., and Hölttä, E. (2000). Caspases and mitochondria in c-Myc-induced apoptosis: identification of ATM as a new target of caspases. Oncogene *19*, 2354–2362.

Isakari, Y., Sogo, S., Ishida, T., Kawakami, T., Ono, T., Taki, T., and Kiwada, H. (2009). Gene expression analysis during platelet-like particle production in phorbol myristate acetate-treated MEG-01 cells. Biol. Pharm. Bull. *32*, 354–358.

Josefsson, E.C., James, C., Henley, K.J., Debrincat, M.A., Rogers, K.L., Dowling, M.R., White, M.J., Kruse, E.A., Lane, R.M., Ellis, S., et al. (2011). Megakaryocytes possess a functional intrinsic apoptosis pathway that must be restrained to survive and produce platelets. J. Exp. Med. *208*, 2017–2031.

Juin, P., Hunt, A., Littlewood, T., Griffiths, B., Swigart, L.B., Korsmeyer, S., and Evan, G. (2002). c-Myc functionally cooperates with Bax to induce apoptosis. Mol. Cell. Biol. *22*, 6158–6169.

Junt, T., Schulze, H., Chen, Z., Massberg, S., Goerge, T., Krueger, A., Wagner, D.D., Graf, T., Italiano, J.E., Jr., Shivdasani, R.A., and von Andrian, U.H. (2007). Dynamic visualization of thrombopoiesis within bone marrow. Science *317*, 1767–1770.

Kaluzhny, Y., Yu, G., Sun, S., Toselli, P.A., Nieswandt, B., Jackson, C.W., and Ravid, K. (2002). BclxL overexpression in megakaryocytes leads to impaired platelet fragmentation. Blood *100*, 1670–1678.

Kumar, S., and Cakouros, D. (2004). Transcriptional control of the core cell-death machinery. Trends Biochem. Sci. *29*, 193–199.

Lambert, M.P., Sullivan, S.K., Fuentes, R., French, D.L., and Poncz, M. (2013). Challenges and promises for the development of donor-independent platelet transfusions. Blood *121*, 3319–3324.

Leytin, V., Allen, D.J., Gwozdz, A., Garvey, B., and Freedman, J. (2004). Role of platelet surface glycoprotein Ibalpha and P-selectin in the clearance of transfused platelet concentrates. Transfusion *44*, 1487–1495.

Lu, S.J., Li, F., Yin, H., Feng, Q., Kimbrel, E.A., Hahm, E., Thon, J.N., Wang, W., Italiano, J.E., Cho, J., and Lanza, R. (2011). Platelets generated from human embryonic stem cells are functional in vitro and in the microcirculation of living mice. Cell Res. *21*, 530–545.

Nakagawa, Y., Nakamura, S., Nakajima, M., Endo, H., Dohda, T., Takayama, N., Nakauchi, H., Arai, F., Fukuda, T., and Eto, K. (2013). Two differential flows in a bioreactor promoted platelet generation from human pluripotent stem cell-derived megakaryocytes. Exp. Hematol. *41*, 742–748.

Nishikii, H., Eto, K., Tamura, N., Hattori, K., Heissig, B., Kanaji, T., Sawaguchi, A., Goto, S., Ware, J., and Nakauchi, H. (2008). Metalloproteinase regulation improves in vitro generation of efficacious platelets from mouse embryonic stem cells. J. Exp. Med. *205*, 1917–1927.

Nishimura, S., Manabe, I., Nagasaki, M., Kakuta, S., Iwakura, Y., Takayama, N., Ooehara, J., Otsu, M., Kamiya, A., Petrich, B.G., et al. (2012). In vivo imaging visualizes discoid platelet aggregations without endothelium disruption and implicates contribution of inflammatory cytokine and integrin signaling. Blood *119*, e45–e56.

Oguro, H., Iwama, A., Morita, Y., Kamijo, T., van Lohuizen, M., and Nakauchi, H. (2006). Differential impact of Ink4a and Arf on hematopoietic stem cells and their bone marrow microenvironment in Bmi1-deficient mice. J. Exp. Med. *203*, 2247–2253.

Ohmine, K., Ota, J., Ueda, M., Ueno, S., Yoshida, K., Yamashita, Y., Kirito, K., Imagawa, S., Nakamura, Y., Saito, K., et al. (2001). Characterization of stage progression in chronic myeloid leukemia by DNA microarray with purified hematopoietic stem cells. Oncogene *20*, 8249–8257.

Okita, K., Yamakawa, T., Matsumura, Y., Sato, Y., Amano, N., Watanabe, A., Goshima, N., and Yamanaka, S. (2013). An efficient nonviral method to generate integration-free human-induced pluripotent stem cells from cord blood and peripheral blood cells. Stem Cells *31*, 458–466.

Ono, Y., Wang, Y., Suzuki, H., Okamoto, S., Ikeda, Y., Murata, M., Poncz, M., and Matsubara, Y. (2012). Induction of functional platelets from mouse and human fibroblasts by p45NF-E2/Maf. Blood *120*, 3812–3821.

Patel, S.R., Hartwig, J.H., and Italiano, J.E., Jr. (2005). The biogenesis of platelets from megakaryocyte proplatelets. J. Clin. Invest. *115*, 3348–3354.

Proulx, C., Dupuis, N., St-Amour, I., Boyer, L., and Lemieux, R. (2004). Increased megakaryopoiesis in cultures of CD34-enriched cord blood cells maintained at 39 degrees C. Biotechnol. Bioeng. *88*, 675–680.

Sato, T., Fuse, A., Eguchi, M., Hayashi, Y., Ryo, R., Adachi, M., Kishimoto, Y., Teramura, M., Mizoguchi, H., Shima, Y., et al. (1989). Establishment of a human leukaemic cell line (CMK) with megakaryocytic characteristics from a Down's syndrome patient with acute megakaryoblastic leukaemia. Br. J. Haematol. *72*, 184–190.

Schiffer, C.A. (2001). Diagnosis and management of refractoriness to platelet transfusion. Blood Rev. *15*, 175–180.

Suemori, H., Yasuchika, K., Hasegawa, K., Fujioka, T., Tsuneyoshi, N., and Nakatsuji, N. (2006). Efficient establishment of human embryonic stem cell lines and long-term maintenance with stable karyotype by enzymatic bulk passage. Biochem. Biophys. Res. Commun. *345*, 926–932.

Takahashi, K., Tanabe, K., Ohnuki, M., Narita, M., Ichisaka, T., Tomoda, K., and Yamanaka, S. (2007). Induction of pluripotent stem cells from adult human fibroblasts by defined factors. Cell *131*, 861–872.

Takayama, N., Nishikii, H., Usui, J., Tsukui, H., Sawaguchi, A., Hiroyama, T., Eto, K., and Nakauchi, H. (2008). Generation of functional platelets from human embryonic stem cells in vitro via ES-sacs, VEGF-promoted structures that concentrate hematopoietic progenitors. Blood *111*, 5298–5306.

Takayama, N., Nishimura, S., Nakamura, S., Shimizu, T., Ohnishi, R., Endo, H., Yamaguchi, T., Otsu, M., Nishimura, K., Nakanishi, M., et al. (2010). Transient activation of c-MYC expression is critical for efficient platelet generation from human induced pluripotent stem cells. J. Exp. Med. *207*, 2817–2830.

Takizawa, H., Nishimura, S., Takayama, N., Oda, A., Nishikii, H., Morita, Y., Kakinuma, S., Yamazaki, S., Okamura, S., Tamura, N., et al. (2010). Lnk regulates integrin alphaIIbbeta3 outside-in signaling in mouse platelets, leading to stabilization of thrombus development in vivo. J. Clin. Invest. *120*, 179–190.

Terui, Y., Furukawa, Y., Kikuchi, J., Iwase, S., Hatake, K., and Miura, Y. (1998). Bcl-x is a regulatory factor of apoptosis and differentiation in megakaryocytic lineage cells. Exp. Hematol. *26*, 236–244.

Ware, J., Russell, S., and Ruggeri, Z.M. (2000). Generation and rescue of a murine model of platelet dysfunction: the Bernard-Soulier syndrome. Proc. Natl. Acad. Sci. USA *97*, 2803–2808.

Wong, C.H., Jenne, C.N., Petri, B., Chrobok, N.L., and Kubes, P. (2013). Nucleation of platelets with blood-borne pathogens on Kupffer cells precedes other innate immunity and contributes to bacterial clearance. Nat. Immunol. *14*, 785–792.

Yamamoto, R., Morita, Y., Ooehara, J., Hamanaka, S., Onodera, M., Rudolph, K.L., Ema, H., and Nakauchi, H. (2013). Clonal analysis unveils self-renewing lineage-restricted progenitors generated directly from hematopoietic stem cells. Cell *154*, 1112–1126.

Yu, M., Mazor, T., Huang, H., Huang, H.T., Kathrein, K.L., Woo, A.J., Chouinard, C.R., Labadorf, A., Akie, T.E., Moran, T.B., et al. (2012). Direct recruitment of polycomb repressive complex 1 to chromatin by core binding transcription factors. Mol. Cell *45*, 330–343.

EUROPEAN JOURNAL OF Haematology

European Journal of Haematology 92 (276–282)

ORIGINAL ARTICLE

TUBB1 mutation disrupting microtubule assembly impairs proplatelet formation and results in congenital macrothrombocytopenia

Shinji Kunishima[1], Satoshi Nishimura[2,3,4], Hidenori Suzuki[5], Masue Imaizumi[6], Hidehiko Saito[7]

[1]Department of Advanced Diagnosis, Clinical Research Center, National Hospital Organization Nagoya Medical Center, Nagoya; [2]Department of Cardiovascular Medicine, The University of Tokyo, Tokyo; [3]Translational Systems Biology and Medicine Initiative, The University of Tokyo, Tokyo; [4]Reserach Division of Cell and Molecular Medicine, Center for Molecular Medicine, Jichi Medical University, Tochigi; [5]Department of Morphological and Biomolecular Research, Graduate School of Medicine, Nippon Medical School, Tokyo; [6]Department of Hematology and Oncology, Miyagi Children's Hospital, Miyagi; [7]Honorary Director, National Hospital Organization Nagoya Medical Center, Nagoya, Japan

Abstract

This report describes a family with *TUBB1*-associated macrothrombocytopenia diagnosed based on abnormal platelet β1-tubulin distribution. A circumferential marginal microtubule band was undetectable, whereas microtubules were frayed and disorganized in every platelet from the affected individuals. Patients were heterozygous for novel *TUBB1* p.F260S that locates at the α- and β-tubulin intradimer interface. Mutant β1-tubulin was not incorporated into microtubules with endogenous α-tubulin, and α-tubulin expression was decreased in transfected Chinese hamster ovary cells. Transduction of mutant β1-tubulin into mouse fetal liver-derived megakaryocytes demonstrated no incorporation of mutant β1-tubulin into microtubules with endogenous α-tubulin and diminished proplatelet formation, leading to the production of fewer, but larger, proplatelet tips. Furthermore, mutant β1-tubulin was not associated with endogenous α-tubulin in the proplatelets. Deficient functional microtubules might lead to defective proplatelet formation and abnormal protrusion-like platelet release, resulting in congenital macrothrombocytopenia.

Key words β1-tubulin; macrothrombocytopenia; microtubules; proplatelet formation; *TUBB1*

Correspondence Shinji Kunishima, PhD, Department of Advanced Diagnosis, Clinical Research Center, National Hospital Organization Nagoya Medical Center, 4-1-1 Sannomaru, Naka-ku, Nagoya 460-0001, Japan. Tel: +81 52 951 1111; Fax: +81 52 951 0664; e-mail: kunishis@nnh.hosp.go.jp

Accepted for publication 12 December 2013

doi:10.1111/ejh.12252

Congenital macrothrombocytopenia is a genetically heterogeneous group of rare platelet disorders, among which *MYH9* disorders/*MYH9*-related disease and Bernard-Soulier syndrome are the most frequent (1–3). Less frequent forms involve defects in signaling pathways and/or components of the cytoskeleton that regulate proplatelet formation and morphology (4, 5). Proplatelets are cytoplasmic extensions of megakaryocytes that are elongated by microtubule-based forces (6). The microtubules are assembled from α- and β-tubulin heterodimers and represent a key component of proplatelet formation and platelet release (7). Expression of the β-tubulin isoform, β1-tubulin, is restricted in megakaryocytes and platelets (8). *Tubb1*-knockout mice show thrombocytopenia and spherical platelets (9). We previously reported the first *TUBB1* mutation affecting microtubule assembly in the context of congenital macrothrombocytopenia (10). Subsequent continuous studies on the differential diagnosis of congenital macrothrombocytopenia detected abnormal β1-tubulin distribution in platelets and revealed a second *TUBB1* mutation that impairs megakaryocyte microtubule organization, proplatelet formation, and platelet morphology.

Materials and methods

Patients

Thrombocytopenia was incidentally identified in 12-year-old dizygotic twin boys (Table 1). Peripheral blood smears

© 2013 John Wiley & Sons A/S. Published by John Wiley & Sons Ltd

Table 1 Characteristics of platelets from a family with *TUBB1* p.F260S mutation

Individual	Sex	Age (years)	*TUBB1* mutation	Platelet count ($\times 10^9$/L)	Platelet size (μm)[1]	Mean platelet volume[2]	Bleeding tendency	Initial diagnosis
Mother	F	37	p.F260S	104	ND	ND	–	Immune thrombocytopenia
Patient 1	M	12	p.F260S	120	3.0 ± 0.9	ND	–	Unknown thrombocytopenia
Patient 2	M	12	p.F260S	97	3.4 ± 0.9	ND	–	Unknown thrombocytopenia
Sister	F	9	p.F260S	125	3.5 ± 0.6	13.8	–	Unknown thrombocytopenia
Mean ± SD				111.5 ± 13.2	3.3 ± 0.3			

[1]Determined by microscopic observation of 200 platelets on a stained peripheral blood smear. Controls, 2.5 ± 0.3 μm (n = 31).
[2]Normal range, 9.4–12.5.

showed large platelets (Fig. 1A). Neither twin had a bleeding tendency. *MYH9* disorders, heterozygous and homozygous Bernard-Soulier syndrome, and glycoprotein (GP) IIb/IIIa-associated macrothrombocytopenia were excluded by immunofluorescence analysis for granulocyte myosin IIA and by flow cytometry for platelet GPIb/IX and GPIIb/IIIa expression, respectively (2, 11). The twins' younger sister also had asymptomatic macrothrombocytopenia. The mother was diagnosed with immune thrombocytopenia, and the father was unavailable for the study. Written informed consent was obtained from the mother in accordance with the Declaration of Helsinki. Institutional Review Boards of Nagoya Medical Center and Miyagi Children's Hospital approved this study.

Immunofluorescence analysis

Peripheral blood smears were fixed with absolute methanol, permeabilized with acetone, double-stained with anti-β1-tubulin antibody NB2301 (1 : 1000)(10) and anti-α-tubulin antibody DM1A (LabVision, Fremont, CA, USA)(1 : 200), and then reacted with Alexa 488-labeled anti-rabbit IgG and Alexa 555-labeled anti-mouse IgG (Invitrogen, Carlsbad, CA, USA). NB2301 was raised in rabbits against a synthetic peptide corresponding to C-terminal 425–451aa of human β1-tubulin. DM1A is a mouse monoclonal antibody raised against native chick brain microtubules. Chinese hamster ovary (CHO) cells transfected with *TUBB1* cDNA and mouse fetal liver-derived megakaryocytes transduced with *TUBB1* cDNA were simultaneously analyzed. Stained cells were examined under a BX50 fluorescence microscope with a 100×/1.35 numerical aperture oil objective using DP Manager software (Olympus, Tokyo, Japan).

Electron microscopy

For transmission electron microscopy, washed platelets prepared from acid-citrate-dextrose citrated whole blood were fixed in 2% glutaraldehyde and postfixed in 1% osmium tetroxide. The platelet samples were embedded in epoxy resin (Epon 812; TAAB, Berks, UK). Ultra-thin sections were cut, stained with uranyl acetate and lead citrate, and observed under a transmission electron microscope (JEM-1010, JEOL, Tokyo, Japan) (12). For negative staining, Triton X-100-extracted platelets were placed on formvar-coated carbon-stabilized grids, stained with uranyl acetate, and examined with JEM-1010 electron microscope (13).

Immunoblot analysis

Whole platelet proteins were isolated using a NucleoSpin RNA/Protein kit (Macherey-Nagel GmbH & Co., KG, Düren, Germany), separated by sodium dodecyl sulfate-polyacrylamide gel electrophoresis on 4–12% gradient acrylamide slab gels (Invitrogen), and electroblotted onto polyvinylidene difluoride membranes. The blots were incubated with anti-αIIb antibody SZ22 (Beckman-Coulter, Miami, FL, USA), DM1A, and NB2301, and reacted with horseradish peroxidase-conjugated secondary antibody. Bound antibodies were visualized using enhanced chemiluminescent substrate. Blots were densitometrically analyzed using ImageQuant software (Molecular Dynamics, Sunnyvale, CA, USA).

Mutational analysis

The entire coding sequence of exons and exon-intron boundaries of *TUBB1* was amplified by PCR, and the products were subjected to DNA sequence analysis as described (10).

Bioinformatic analysis

The multiple alignment of β1-tubulin was processed using the ClustalW program (http://www.clustal.org). The potential functional effects of the mutation was predicted using different function prediction programs, such as PROVEAN (http://www.provean.jcvi.org), Mutation Taster (http://www.mutationtaster.org), and PolyPhen2 (http://genetics.bwh.harvard.edu/pph2/). The 3D structure of β-tubulin was generated with the program MacPyMol (http://www.delanoscientific.com/) with coordinates from Protein Data Base entry 1JFF (http://www.pdb.org/).

TUBB1 transfection

TUBB1 cDNA in-frame with the C-terminal myc epitope tag cloned into pcDNA3.1 (pcDNA3.1/*TUBB1*myc)

© 2013 John Wiley & Sons A/S. Published by John Wiley & Sons Ltd

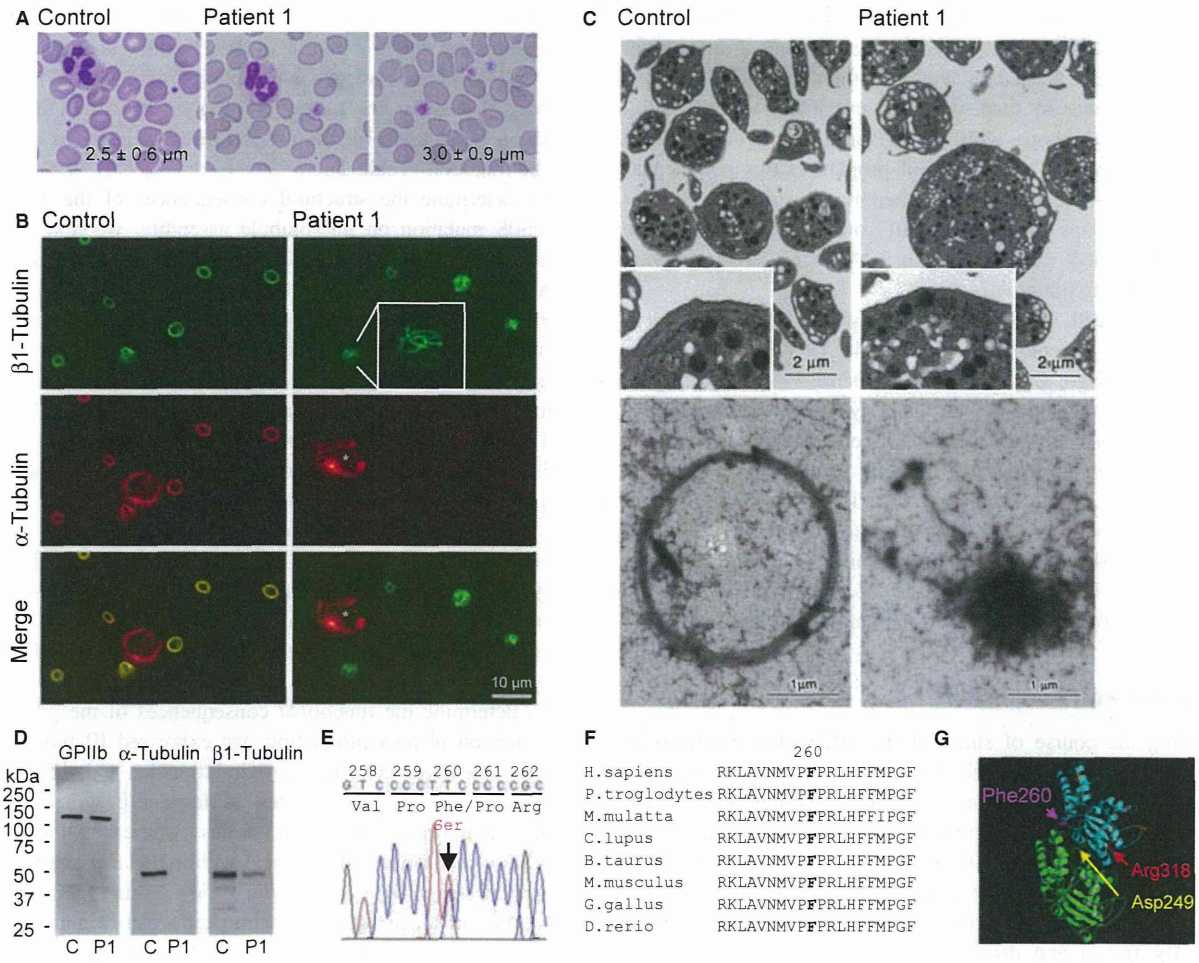

Figure 1 Platelet microtubule organization and β1-tubulin (A) Platelet morphology. Peripheral blood smears were stained with May-Grünwald Giemsa (original magnification, ×1000). The patient showed giant platelets with morphologically normal leukocytes. Numbers in each panel indicate mean platelet size (μm; $n = 200$). (B) Immunofluorescence analysis of platelet tubulin. Platelets from patient 1 lack marginal band structure, and frayed and disorganized microtubule-like structures were evident. Asterisks indicate leukocytes stained for α-tubulin. (C) Ultrastructure of platelets. Upper panels: Conventional transmission electron microscopy. Circumferential microtubules are absent in marginal region of the platelets from patient 1 (Inset). Lower panels: Negative staining. Circumferential microtubule coil was absent in the platelets from patient 1. (D) Immunoblot analysis of platelet tubulin. C, control; P1, patient 1. (E) Entire coding sequence of exons and exon-intron boundaries of *TUBB1* was amplified by PCR and subjected to direct cycle sequence analysis. A T to C transition at nucleotide 779 (c.779T > C), changing Phe260 to Ser (p.F260S), was detected. Arrow indicates position of substitution. (F) Multiple alignment of β1-tubulin. Amino acid sequence alignment of β1-tubulin is shown for human and other species. Substituted amino acid is indicated in bold. (G) Structural analysis of p.F260S using a tubulin 3D model. Arrows indicate locations of p.F260S, p.D249N, and p.R318W. Phe260 (magenta) and Asp249 (yellow) are located at, and Arg318 (red) is located near α and β intradimer interface. Blue, β-tubulin; green, α-tubulin.

(Invitrogen) was described previously (10). p.F260S mutant construct was prepared on pcDNA3.1/*TUBB1*myc by site-directed mutagenesis. CHO cells were transiently transfected with pcDNA3.1/*TUBB1*myc. At 24 h post-transfection, cells were seeded on fibronectin-coated (10 μg/mL) chamber slides (Millipore, Bedford, MA, USA) and cultured for 3 h. They were subjected to immunofluorescence analysis.

Retroviral transduction of cultured megakaryocytes

TUBB1 cDNA with the C-terminal myc epitope tag (*TUBB1*myc) was subcloned into the retroviral vector, pGCDNsamIRES/EGFP, and transfected into 293gpg packaging cells to obtain viral stocks (11, 14). Particles were pseudotyped using vesicular stomatitis virus G protein. E13.5 mouse fetal liver cells were transduced with wild type

© 2013 John Wiley & Sons A/S. Published by John Wiley & Sons Ltd

or p.F260S mutant pGCDNsamIRES/EGFP-*TUBB1*myc and cultured with 40 ng/mL of recombinant mouse thrombopoietin. Proplatelet formation was monitored on EGFP-positive megakaryocytes in suspension cultures under an IX71 fluorescence microscope with an LCPlanFI 20×/0.40 objective lens (Olympus). The number of proplatelet tips per megakaryocyte was counted on acquired images, and the size of proplatelet tips was measured on immunofluorescence images stained with NB2301 using ImageJ 1.43u software (http://rsb.info.nih.gov/ij).

For live-cell imaging experiments, the cells were incubated with PE-conjugated anti-CD41 (MWReg30, Biolegend, San Diego, CA, USA) and Hoechst 33342 (Invitrogen) to identify megakaryocytes. The dynamics of megakaryocytes (proplatelet formation and cell rupture) cultured at 37°C were visualized using an A1R confocal laser scanning microscope with a PlanApo 100×/1.40 numerical aperture oil objective using three laser lines (405, 488, and 561 nm) (Nikon Instruments, Tokyo, Japan). The Experimental Animal Committee of Nagoya Medical Center and the University of Tokyo approved the animal studies.

Results and discussion

During the course of study of the differential diagnosis of congenital macrothrombocytopenia, immunofluorescence analysis detected abnormal β1-tubulin distribution in platelets from a family comprising male twins, their sister, and mother. In resting normal platelets, β1-tubulin is localized in the marginal microtubule band. In contrast, the circumferential ring staining was absent, whereas microtubules were clearly frayed and disorganized in every platelet from the affected individuals (Fig. 1B). Faint immunofluorescence staining indicated reduced levels of α-tubulin in platelets from patients compared with those from control patients observed under the same conditions. Under transmission microscopy, circumferential microtubules were identified lying just inside cell membrane in equatorial plane of the control platelets. In contrast, round and large platelets are evident in samples from patient 1; circumferential microtubules are absent in marginal region. Negative stain electron microscopy demonstrated organized circumferential microtubule coils, comprising about 10 microtubules in control platelets. Circumferential microtubule coil was absent in the platelets from patient 1. Microtubule coil possesses a single, straight, free end, and spreads from center of an electron-dense platelet (Fig. 1C). The expression of platelet β1-tubulin was decreased by 38%, and that of α-tubulin was decreased to 2% compared with that in control platelets (Fig. 1D). The decrease was not accompanied by a decrease of mRNA levels (data not shown).

We searched for *TUBB1* mutations and found a novel conserved p.F260S (c.779T > C) mutation located at the α- and β-tubulin intradimer interface (Fig. 1E–G)(15). Restriction analysis confirmed heterozygosity in the affected individuals. The mutation was not found in 108 healthy controls or in the SNP database (http://www.ncbi.nlm.nih.gov/SNP/), suggesting that it is not a common polymorphism. Different function prediction programmes suggested deleterious effects of the mutation (Table 2).

To determine the structural consequences of the *TUBB1* p.F260S mutation on microtubule assembly, we first monitored mutant β1-tubulin in CHO cells after transient transfection (Fig. 2A). Wild-type β1-tubulin was localized as fine filamentous cytoplasmic networks, indicating incorporation of recombinant β1-tubulin into microtubules with endogenous α-tubulin. In contrast, mutant β1-tubulin was not incorporated into microtubules, and the distribution was diffuse and partly perinuclear. Expression of β1-tubulin in CHO cells has been reported to arrest mitosis and lead to the formation of large multinucleated cells (16). The CHO cells became larger, multinucleated, and polyploid, and these effects were more prominent in the mutant-transfected cells (Fig. 2A). The expression of endogenous α-tubulin was decreased within the mutant-transfected cells, which was similar to the findings observed in platelets (Figs 1B,D and 2A).

To determine the functional consequences of the p.F260S mutation on platelet production, we expressed β1-tubulin in mouse fetal liver cells by retroviral transfer and differentiated them into megakaryocytes. Wild-type β1-tubulin was finely incorporated into microtubules, whereas mutant β1-tubulin was diffusely distributed within the megakaryocyte cytoplasm (Fig. 2B). During the 4-day culture period, the proportion of megakaryocytes with proplatelet formation was decreased among megakaryocytes transduced with the mutant. The number of proplatelet tips was decreased, and the size of the tips increased (Fig. 2C,D). Live-cell imaging showed that the extent of proplatelet formation was clearly diminished. Proplatelet elaboration was scarcely observed, and instead, large bleb protrusions were occasionally evident in mutant-transduced megakaryocytes (Fig. 2D and Video S1, S2). These findings indicated that the mutant β1-tubulin dominantly affected the microtubule assembly and impaired proplatelet formation.

Dynamic microtubule assembly and polymerization are required to regulate proplatelet formation and platelet maturation (7, 17). The coordinate levels of α- and β-tubulins are

Table 2 Functional prediction for *TUBB1* p.F260S mutation

	PROVEAN	Mutation taster	PolyPhen2
Prediction	Deleterious	Disease causing	Probably damaging
Score	−6.794	4.23	

The potential functional effects of the mutation were predicted using different function prediction programs.

© 2013 John Wiley & Sons A/S. Published by John Wiley & Sons Ltd

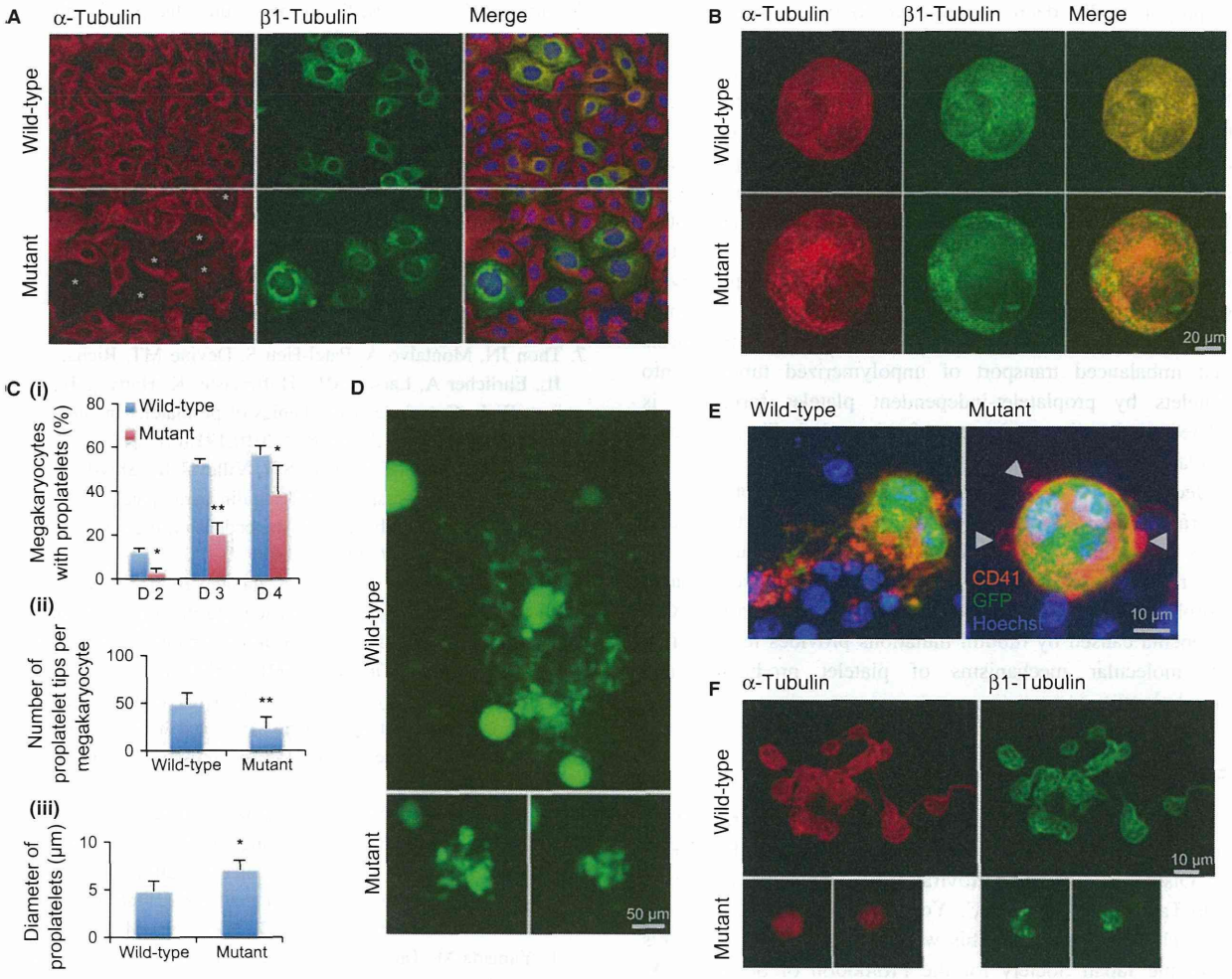

Figure 2 β1-tubulin transduction in Chinese hamster ovary (CHO) cells and mouse fetal liver-derived megakaryocytes. (A) β1-tubulin localization in CHO cells that were transiently transfected with pcDNA3.1/*TUBB1*myc. Cells were stained with antibodies to endogenous α-tubulin (red) and to the transfected β1-tubulin (green) as well as DAPI to label the DNA (blue). In merged images, CHO cells expressing wild-type β1-tubulin appear as yellow or orange, whereas cells expressing mutant β1-tubulin appear green because the expression of endogenous α-tubulin was decreased (asterisks). Cells are representative of five independent experiments. (B) Microtubule organization in β1-tubulin-transduced megakaryocytes. Cells were stained endogenous α-tubulin with DM1A (red) and the transduced β1-tubulin with anti-myc antibody (MBL, Nagoya, Japan) (green). Wild-type β1-tubulin was incorporated into microtubules, but mutant β1-tubulin was not. (C) Abnormal proplatelet formation in β1-tubulin-transduced megakaryocytes. (i) The percentage of megakaryocytes extending proplatelets was decreased in mutant-transduced cells. For each sample, 100 megakaryocytes were evaluated. (ii) The number of proplatelet tips per megakaryocyte was decreased in mutant-transduced cells. Fifty megakaryocytes per sample were evaluated. (iii) Size of proplatelet tips was increased in mutant-transduced cells. One hundred EGFP and β1-tubulin double-positive proplatelet tips per sample were evaluated. Data were analyzed using unpaired, two-tailed t-tests. $P < 0.05$ was considered statistically significant. Data are presented as mean ± SD. $^{*}P < 0.05$, $^{**}P < 0.001$. (D) Representative megakaryocytes extending proplatelets from three independent experiments. Fewer proplatelet tips/bulbous structures are evident, and size of tips is increased in megakaryocytes transduced with mutant. (E) Representative megakaryocytes from three independent live-cell imaging experiments. Megakaryocytes were differentiated from fetal liver cells of CAG-eGFP mice; therefore, the cytoplasm can be identified by eGFP signals (green). The cells were stained with Hoechst to identify nucleus (blue) and anti-CD41 antibody (red). Proplatelet elaboration is rare, and occasional large bleb protrusions are evident in megakaryocytes transduced with mutant (arrow heads). Original videos are available as Video S1 and S2. (F) Microtubule organization in proplatelet tips. Megakaryocyte cultures were cytospun on glass slides. Representative images from three independent experiments.

transcriptionally and translationally maintained for proper heterodimer assembly in cells, and when exogenous β-tubulin is overexpressed, the synthesis of the endogenous β-tubulin is inhibited and that of α-tubulin is upregulated (18, 19). The synthesis of β2- and β5-tubulins was increased in *TUBB1*-knockout mice (9). In contrast, α-tubulin was

© 2013 John Wiley & Sons A/S. Published by John Wiley & Sons Ltd

disproportionally decreased relative to the decrease in β1-tubulin (Fig. 1B,D), and furthermore, β5-tubulin was substantially absent in our patients' platelets (data not shown). Defective mutant β1-tubulin would cause deregulated microtubule organization, as shown in platelets, CHO cells, and cultured megakaryocytes and proplatelet tips (Figs 1B and 2A,B,F). Thus, the deficient functional microtubules might lead to defective proplatelet formation and abnormal protrusion-like platelet release (Fig. 2D,E, Video S2). Defective microtubule organization and proplatelet formation were recently documented in Rac1- and Cdc42-deficient mice (20). Combined, these observations support the hypothesis that imbalanced transport of unpolymerized tubulins into platelets by proplatelet-independent platelet formation is related to the disorganization of microtubule-like structures in platelets.

Because p.D249N and p.R318W, locating at or near the interface, also reportedly cause macrothrombocytopenia in dogs and humans, respectively, mutations disrupting the structure of the intradimer interface might affect platelet morphology (10, 21). Analysis of congenital macrothrombocytopenia caused by tubulin mutations provides insights into the molecular mechanisms of platelet production and morphology.

Acknowledgements

The authors would like to thank R.C. Mulligan for 293gp and 293gpg cells, M. Onodera for pGCDNsamIRES/EGFP, M. Otsu for help with retroviral experiments, as well as Y. Kito-Takagi, M. Tajima, C. Yoshinaga, and T. Hirabayashi for technical assistance. This work was supported by grants from the Japan Society for the Promotion of Science KAKENHI (S.K.), Mitsubishi Pharma Research Foundation (S.K.), the 24th General Assembly of the Japanese Association of Medical Sciences (S.K.), Funding Program for Next Generation World-Leading Researchers (S.N.), and the Translational Systems Biology, Medicine Initiative (S.N.) from the Japan Science and Technology Agency.

Authorship and disclosures

S.K. designed and performed research, analyzed data, and wrote the paper; S.N. performed live-cell imaging experiments; H. Suzuki performed electron microscopic analysis; M.I. contributed patient samples; H. Saito supervised the research. The authors report no potential conflict of interests.

References

1. Balduini CL, Savoia A. Genetics of familial forms of thrombocytopenia. *Hum Genet* 2012;**131**:1821–32.
2. Kunishima S, Saito H. Congenital macrothrombocytopenias. *Blood Rev* 2006;**20**:111–21.
3. Nurden AT, Freson K, Seligsohn U. Inherited platelet disorders. *Haemophilia* 2012;**18**(Suppl 4):154–60.
4. Thon JN, Italiano JE Jr. Does size matter in platelet production? *Blood* 2012;**120**:1552–61.
5. Thon JN, Macleod H, Begonja AJ, Zhu J, Lee KC, Mogilner A, Hartwig JH, Italiano JE Jr. Microtubule and cortical forces determine platelet size during vascular platelet production. *Nat Commun* 2012;**3**:852.
6. Italiano JE Jr, Lecine P, Shivdasani RA, Hartwig JH. Blood platelets are assembled principally at the ends of proplatelet processes produced by differentiated megakaryocytes. *J Cell Biol* 1999;**147**:1299–312.
7. Thon JN, Montalvo A, Patel-Hett S, Devine MT, Richardson JL, Ehrlicher A, Larson MK, Hoffmeister K, Hartwig JH, Italiano JE Jr. Cytoskeletal mechanics of proplatelet maturation and platelet release. *J Cell Biol* 2010;**191**:861–74.
8. Lecine P, Italiano JE Jr, Kim SW, Villeval JL, Shivdasani RA. Hematopoietic-specific β1 tubulin participates in a pathway of platelet biogenesis dependent on the transcription factor NF-E2. *Blood* 2000;**96**:1366–73.
9. Schwer HD, Lecine P, Tiwari S, Italiano JE Jr, Hartwig JH, Shivdasani RA. A lineage-restricted and divergent β-tubulin isoform is essential for the biogenesis, structure and function of blood platelets. *Curr Biol* 2001;**11**:579–86.
10. Kunishima S, Kobayashi R, Itoh TJ, Hamaguchi M, Saito H. Mutation of the β1-tubulin gene associated with congenital macrothrombocytopenia affecting microtubule assembly. *Blood* 2009;**113**:458–61.
11. Kunishima S, Kashiwagi H, Otsu M, *et al.* Heterozygous ITGA2B R995W mutation inducing constitutive activation of the αIIbβ3 receptor affects proplatelet formation and causes congenital macrothrombocytopenia. *Blood* 2011;**117**:5479–84.
12. Suzuki H, Kaneko T, Sakamoto T, Nakagawa M, Miyamoto T, Yamada M, Tanoue K. Redistribution of α-granule membrane glycoprotein IIb/IIIa (integrin αIIbβ3) to the surface membrane of human platelets during the release reaction. *J Electron Microscopy* 1994;**43**:282–9.
13. White JG, Krumwiede M. Isolation of microtubule coils from normal human platelets. *Blood* 1985;**65**:1028–32.
14. Kunishima S, Okuno Y, Yoshida K, *et al.* ACTN1 mutations cause congenital macrothrombocytopenia. *Am J Hum Genet* 2013;**92**:431–8.
15. Lowe J, Li H, Downing KH, Nogales E. Refined structure of αβ-tubulin at 3.5 a resolution. *J Mol Biol* 2001;**313**:1045–57.
16. Yang H, Ganguly A, Yin S, Cabral F. Megakaryocyte lineage-specific class VI β-tubulin suppresses microtubule dynamics, fragments microtubules, and blocks cell division. *Cytoskeleton* 2011;**68**:175–87.
17. Patel-Hett S, Richardson JL, Schulze H, *et al.* Visualization of microtubule growth in living platelets reveals a dynamic marginal band with multiple microtubules. *Blood* 2008;**111**:4605–16.
18. Cleveland DW. Autoregulated instability of tubulin mRNAs: a novel eukaryotic regulatory mechanism. *Trends Biochem Sci* 1988;**13**:339–43.

© 2013 John Wiley & Sons A/S. Published by John Wiley & Sons Ltd

19. Gonzalez-Garay ML, Cabral F. Overexpression of an epitope-tagged β-tubulin in Chinese hamster ovary cells causes an increase in endogenous alpha-tubulin synthesis. *Cell Motil Cytoskeleton* 1995;**31**:259–72.
20. Pleines I, Dutting S, Cherpokova D, *et al.* Defective tubulin organization and proplatelet formation in murine megakaryocytes lacking Rac1 and Cdc42. *Blood* 2013;**122**:3178–87.
21. Davis B, Toivio-Kinnucan M, Schuller S, Boudreaux MK. Mutation in β1-tubulin correlates with macrothrombocytopenia in Cavalier King Charles Spaniels. *J Vet Intern Med* 2008;**22**:540–5.

Supporting Information

Additional Supporting Information may be found in the online version of this article:

Video S1. Live-cell imaging of platelet release. Original movie of Figure 2E (left, wild type).

Video S2. Live-cell imaging of platelet release. Original movie of Figure 2E (right, mutant).

© 2013 John Wiley & Sons A/S. Published by John Wiley & Sons Ltd

Exp. Anim. 63(4), 475–481, 2014

—Original—

A Long-term Follow-up Study on the Engraftment of Human Hematopoietic Stem Cells in Sheep

Tomoyuki ABE [1, 2], Yutaka HANAZONO [1, 3], and Yoshikazu NAGAO [2]

[1] *Division of Regenerative Medicine, Center for Molecular Medicine, Jichi Medical University, 3311-1 Yakushiji, Shimotsuke-shi, Tochigi 329-0498, Japan*
[2] *University Farm, Department of Agriculture, Utsunomiya University, 443 Shimokomoriya, Mouka-shi, Tochigi 321-4415, Japan*
[3] *CREST, Japan Science and Technology Agency, 5-3 Yonbancho, Chiyoda-ku, Tokyo 102-8666, Japan*

Abstract: Xenograft models of human hematopoiesis are essential to the study of the engraftment and proliferative potential of human hematopoietic stem cells (HSCs) *in vivo*. Immunodeficient mice and fetal sheep are often used as xenogeneic recipients because they are immunologically naive. In this study, we transplanted human HSCs into fetal sheep and assessed the long-term engraftment of transplanted human HSCs after birth. Fourteen sheep were used in this study. In 4 fetal sheep, HSCs were transduced with homeo-box B4 *(HOXB4)* gene before transplantation, which promoted the expansion of HSCs. Another 4 fetal sheep were subjected to non-myeloablative conditioning with busulfan. Seven of these 8 sheep showed successful engraftment of human HSCs (1–3% of colony-forming units) as assessed after the birth of fetal sheep (5 months post-transplantation), although *HOXB4*-transduced HSCs showed sustained engraftment for up to 40 months. Intact HSCs were transplanted into six non-conditioned fetal sheep, and human colony-forming units were not detected in the sheep after birth. These results suggest that, as compared with mouse models, where the short lifespan of mice limits long-term follow-up of HSC engraftment, the fetal sheep model provides a unique perspective for evaluating long-term engraftment and proliferation of human HSCs.
Key words: engraftment, hematopoietic stem cells, large animal models, long-term follow-up, sheep

Introduction

Animal transplantation models are indispensable for functional assessment of hematopoietic stem cells (HSCs), because reliable *in vitro* surrogate assays for the cells capable of long-term hematopoietic repopulation *in vivo* are currently unavailable [8, 11]. As experimental transplantation of HSCs into humans is ethically unattainable, xenograft models are commonly used for studying engraftment and proliferative potential of human HSCs *in vivo*. Several xenogeneic transplantation models have been studied, of which immunodeficient mice [5–7, 9, 15] and fetal sheep [31] are advantageous because of their immunologically naive state. Human HSCs can readily engraft and generate progeny in these animals. Although immunodeficient mice have gained the broadest application in laboratory research due to the ease of access and handling of animals, humans and mice show distinct differences, especially in lifespan and body size, which are relevant to HSC transplantation. The reconstitution of human hematopoiesis in mice allows for observation for 1–2 y after serial transplantation [10, 16, 29]; however, execution of the procedure requires a large number of mice (Fig. 1).

The aim of this study was to examine whether the transplantation of human HSCs into fetal sheep could

(Received 22 April 2014 / Accepted 28 May 2014 / Published online in J-STAGE 22 July 2014)
Address corresponding: Yutaka Hanazono (MD, PhD), Division of Regenerative Medicine, Center for Molecular Medicine, Jichi Medical University, 3311-1 Yakushiji, Shimotsuke-shi, Tochigi 329-0498, Japan

©2014 Japanese Association for Laboratory Animal Science

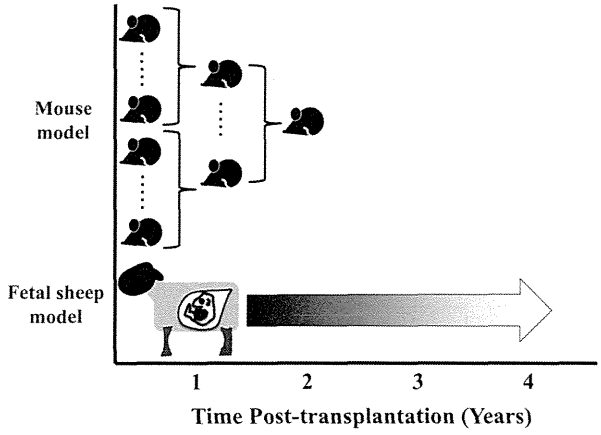

Fig. 1. Long-term assessment of human HSCs *in vivo*. In immunodeficient mice, although serial transplantation is an approach to evaluate the long-term assessment of human hematopoietic stem cells (HSCs), a large number of mice are required for the following transplantation. In contrast in sheep, the long-term assessment can be achieved in single animals. It is possible to conduct repeated bleeding and evaluation of samples at desired intervals over long periods without serial transplantation in sheep.

allow long-term engraftment of the cells in the sheep after birth. Long-term assessment of human HSCs in sheep can be performed because the large size and long lifespan of sheep allow repeated sampling of bone marrow (BM) in individual animals at desired intervals for long periods of time [1, 24, 31]. Here we report sustained engraftment of human HSCs in sheep for up to 40 months post-transplantation as assessed by clonogenic assays of the BM.

Materials and Methods

Animals

Pregnant Suffolk ewes (Japan Lamb, Hiroshima, Japan) were bred at Jichi Medical University and at Utsunomiya University Farm. All experiments in this study were performed in accordance with the Jichi Medical University Guide for Laboratory Animals and the Utsunomiya University Guide for Experimental Animals.

Graft preparation

Human cord blood (CB) was supplied by the RIKEN BioResource Center Cell Bank (Ibaraki, Japan). Human CB $CD34^+$ cells, used as hematopoietic stem cells (HSCs), were isolated by immunomagnetic separation using an anti-human CD34 microbeads kit (Miltenyi Biotech, Auburn, CA, USA) according to the manufacturer's instructions. In a protocol (4 out of the 14 CB samples), namely *HOXB4* protocol, human CB $CD34^+$ cells were transduced before transplantation with a polymerase gene-defective Sendai virus vector (DNAVEC Corp., Ibaraki, Japan) that transiently expressed the human *HOXB4* gene (GenBank accession No. NM 024015). The *HOXB4* gene provided a selective growth advantage to transduced HSCs *in vivo* [4, 25, 26, 32]. The transduction was conducted by culturing the cells for 4 days in the presence of 100 ng/ml recombinant human (rh) stem cell factor (SCF), rh Flt3 ligand (both from R&D Systems, Minneapolis, MI, USA) and rh thrombopoietin (Kyowa Hakko-Kirin Co., Ltd., Tokyo, Japan) [1].

In utero transplantation (IUT)

The cells were transplanted into the liver of fetal sheep at 45 to 49 days of gestation (full term, 147 days). The procedures of IUT were described previously [17]. In another protocol (the BU protocol), some fetuses (4 out of the 14 sheep) received busulfan (BU, Wako Pure Chemical Industries Ltd., Osaka, Japan) via the dams intravenously at 3 mg/kg (calculated based on maternal body weight) 6 days before transplantation [2]. BU is often administered to patients as a conditioning agent before HSC transplantation [3, 21].

Colony-forming unit (CFU) assay

CB $CD34^+$ cells used for transplantation or sheep bone marrow (BM) cells post-transplantation were subjected to CFU assay. Briefly, cells were plated in a 35-mm petri dish with 1 ml of MethoCult GF^+ H4435 (StemCell Technologies, Vancouver, BC, Canada) containing SCF, granulocyte colony-stimulating factor (G-CSF), granulocyte-macrophage CSF, interleukin (IL)-3, IL-6 and erythropoietin, which were recombinant human products and purchased from StemCell Technologies. The culture conditions equivalently support the growth of ovine as well as human CFUs, and thus no difference in the efficiency of colony formation between ovine and human hematopoietic cells was observed in this assay [24]. After incubation at 37°C with 5% CO_2 for 14 days, colonies containing more than 50 cells were counted under an inverted light microscope [1, 2]. Statistical significance of the difference in colony numbers was determined by the ANOVA-test.

Table 1. Long-term engraftment in sheep after in-utero transplantation of human hematopoietic stem cells

Protocols	Animal no.	In utero transplantation			Engraftment (% of human CFUs)[a]				
		Gestational day of transplant (Full term: 147 days)	Number of transplanted cells per fetus ($\times 10^5$)	Number of transplanted $CD34^+$ cells per fetus ($\times 10^5$)	5 months post IUT	15–17 months post IUT	20–25 months post IUT	40 months post IUT	58 months post IUT
HOXB4[b]	Y705-1	49	5.2	3.8	0.0	0.0	0.0	-	
	Y705-2	49	4.5	4.5	1.1	2.2	2.2	2.2	0.0
	Y271-1	49	3.2	2.9	3.3	1.1	0.0	-	
	Y271-2	49	8.9	7.6	2.2	0.0	0.0	-	
BU[c]	Y940-1	48	20.0	17.5	1.1	-[e]			
	Y940-2	48	20.1	13.8	1.1	-	0.0	-	
	Y1061-1	48	7.2	2.8	2.2	0.0	-		
	Y1061-2	48	10.7	5.8	3.3	0.0	-		
Non-treatment[d]	Y1018-1	49	23.6	17.8	0.0	-			
	Y1018-2	49	15.5	12.0	0.0	-			
	Y973	45	8.6	5.6	0.0	-			
	Y936	47	7.3	5.4	0.0	-			
	W110	48	17.7	13.7	0.0	-			
	Y955	48	13.3	10.1	0.0	-			

[a] Percentage of human CFUs was calculated by dividing the number of CFUs positive for the human-specific *β2-microglobulin* gene sequence by the total number of CFUs being analyzed in the bone marrow. [b] In the *HOXB4* protocol, human $CD34^+$ cells transduced with *HoxB4* were transplanted into non-con ditioned fetal sheep [1]. [c] In the BU protocol, BU was administered 6 days before IUT of non-transduced human $CD34^+$ cells [2]. [d] In the non-treatment protocol, non-transduced human $CD34^+$ cells were transplanted into non-conditioned fetal s heep [1, 2]. [e] Sheep Y940-1 unexpectedly died from an accident during the procedures of bone marrow aspiration. CFU, colony-forming unit; BU, busulfan; IUT, in utero transplantation.

Assessment of human engraftment

To evaluate the engraftment of human cells, BM was aspirated from the iliac bone of lambs using a 13-gauge biopsy needle (Jamshidi, CareFusion, San Diego, USA), under local anesthesia with 2% lidocain (Xylocaine, AstraZeneca, Tokyo, Japan). BM cells were harvested by removing red blood cells with ACK lysis buffer (155 mM NH_4Cl, 100 mM $KHCO_3$, and 1 mM EDTA) (Wako Pure Chemical Industries, Ltd.). *In vitro* colony formation assay of sheep BM cells after transplantation was conducted as described above (in the section of *CFU assay*). Each colony was derived from a single human or sheep hematopoietic progenitor cell. DNA of each colony was subjected to polymerase chain reaction (PCR) to identify human colonies [24]. First, each colony was plucked into 50 μl of distilled water and digested with 20 μg/ml proteinase K (Takara, Shiga, Japan) at 55°C for 2 h, followed by 99°C for 10 min, to extract DNA. Each DNA sample (5 μl) was used for a nested PCR to identify the human β2-microglobulin–specific sequences [1, 2]. The outer primer set was 5′-CAGGTTTACTCACGTCATCCAG-3′ and 5′-GGTTCACACGGCAGGCATACTC-3′, and the inner primer set was 5′-GTCTGGGTTTCATCCATCCG-3′ and 5′- GGTGAATTCAGTGTAGTACAAG-3′. The amplification conditions for the outer PCR were 95°C for 30 s, 58°C for 30 s, and 72°C for 30 s for 25 cycles. The outer PCR products were purified using a QIA quick PCR purification kit (Qiagen, Chatsworth, CA, USA). The amplification conditions for the inner PCR were 95°C for 30 s, 58°C for 30 s, and 72°C for 30 s for 30 cycles. Simultaneous PCR for the β-actin sequence was also performed to verify the DNA amplification of each sample. The primer sequences of either humans or sheep were 5′-GTCACCCACACTGTGCCCATCTACG-3′ and 5′-GCCATCTCCTGCTCGAAGTC-3′. The amplification conditions were 94°C for 30 s, 55°C for 30 s, and 72°C for 30 s for 40 cycles. The amplified human β2-microglobulin (133 bp) and β-actin (209 bp) products were resolved by 2% agarose gel and visualized by ethidium bromide staining. The engraftment efficiency of human hematopoietic cells was expressed as the ratio of the number of human-derived colonies to the total number of colonies.

Results

Frozen human cord blood (CB) was obtained from RIKEN Cell Bank. The cells were thawed, and a range of $2.8 \times 10^5 - 17.8 \times 10^5$ of $CD34^+$ cells were isolated

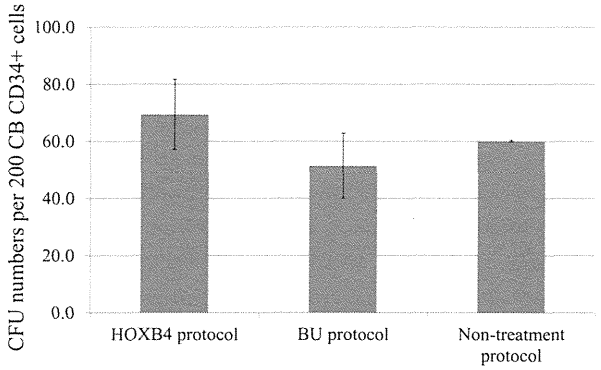

Fig. 2. *In vitro* CFU assay for validating the viability and functionality of transplanted CD34$^+$ cells. In order to assess the viability and functionality of human cord blood (CB) CD34$^+$ cells in the three protocols, colony forming-unit (CFU) assays of each CB CD34$^+$ sample were conducted. Results are shown as mean ± standard deviation. Statistical significance was determined by ANOVA test. No significant difference was observed among the three protocols.

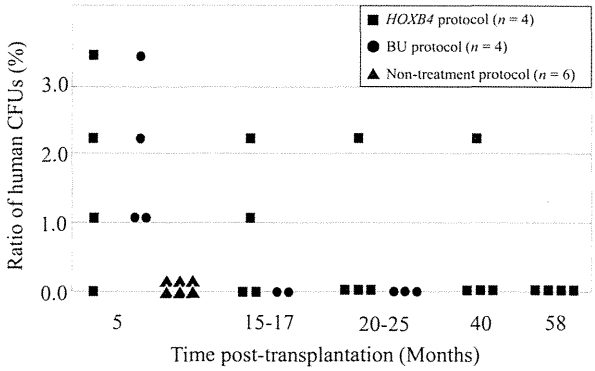

Fig. 3. Long-term follow-up of human HSC engraftment after IUT in sheep. Human cord blood (CB) CD34$^+$ cells were transduced with *HOXB4* and transplanted into intact (non-conditioned) fetal sheep (*HOXB4* protocol, ■). Intact (non-transduced) human CB CD34$^+$ cells were transplanted into fetal sheep conditioned with busulfan (BU) (BU protocol, ●). In addition, intact human CB CD34$^+$ cells were transplanted into intact fetal sheep (non-treatment protocol, ▲). The scatter plots show percentages of human colony-forming units (CFUs) at the indicated months after in utero transplantation (IUT). The percentage of human CFUs was calculated by dividing the number of CFUs expressing the human β2-microglobulin gene by the total number of CFUs being analyzed in the bone marrow.

for use as hematopoietic stem cells (HSCs) for transplantation in fetal sheep. The cells were transplanted into 14 fetal sheep at 45 to 49 days of gestation. Two protocols were used in some of the sheep [1, 2]. Four fetal sheep received *HOXB4*-transduced CD34$^+$ cells (the *HOXB4* protocol) [1]. Another 4 fetal sheep were subjected to non-myeloablative conditioning with busulfan (the BU protocol) [2]. The two protocols, which exhibited comparable effects on the short-term engraftment potential of HSCs (up to 5 months post-transplantation) [1, 2].

The number of transplanted CD34$^+$ cells varied widely among the 14 sheep from 2.8×10^5 to 17.8×10^5, and the maximal cell number was about 6.4 times larger than the minimum cell number (Table 1). However, the numbers of mononuclear cells and CD34$^+$ cells that were transplanted into each fetus did not differ significantly among the three protocols (Table 1; P=0.06 and 0.14, respectively).

To verify the viability and functionality of the transplanted cells, we performed CFU assays and compared the results of the two modified protocols and the original protocol (Fig. 2). The CB CD34$^+$ cells formed multilineage colonies (CFU-G, M, GM and BFU-E) at similar efficiencies as those shown in other previous reports [7, 22, 23]. There was no significant difference in the number of CFUs among the three protocols (P=0.09), suggesting comparable viability and functionality of CB CD34$^+$ cells transplanted in all three protocols in the present study. Regarding the *HOXB4* protocol, the transduction of CB CD34$^+$ cells with the *HOXB4* gene did not affect the myeloid/erythroid ratio as assessed by CFU assays. It was about 10:1 either before or after the *HOXB4* transduction.

A total of 14 ovine fetuses received transplantation, and no abortion was observed in this study. After the birth of lambs, the BM of each lamb was tested to identify the presence of human CFUs (Table 1). In the non-treatment group, human CFUs were not detected after birth [1, 2]. In the BU protocol, human CFUs were detected up to 5 months post-transplantation [2]. Notably, in the *HOXB4* protocol, they were detectable up to 40 months post-transplantation (Fig. 3). All of the sheep lost human CFUs by 58 months post-IUT. Thus, human hematopoietic cells could engraft in sheep for up to 40 months. However, extremely low levels (<0.01%) of transplant-derived cells were detected in the peripheral blood (PB) of all of the sheep, in good agreement with the results in our previous studies and other reports [1, 2, 18–21, 24, 28, 30].

Discussion

In this study, we showed long-term engraftment of human HSCs in sheep for up to 40 months through the *HOXB4* protocol; that is, we detected human clonogenic hematopoietic colonies in sheep BM for the period. Previous other studies just showed the presence of human cells in the PB by flow cytometry with anti-human CD45 antibody or other human specific hematopoietic markers, but did not conduct clonogenic studies [31]. This is the first report showing the evidence of long-term engraftment of human HSCs in sheep through clonogenic assays.

In the original non-treatment protocol of our sheep IUT (i.e., without genetic transduction or conditioning), human CB $CD34^+$ cells could not mediate engraftment for longer than 5 months post-transplantation [1, 2]. However, Zanjani *et al.* [31] demonstrated successful cell engraftment for up to 3.6 y after the transplantation of human fetal liver HSCs even without genetic transduction or conditioning. There are several possible explanations for this discrepancy, one of which is the route of injection. Zanjani *et al.* [31] injected cells into the abdominal cavity of fetal sheep, whereas we injected cells into the liver of fetal sheep. However, we previously showed that no significant differences in the engraftment efficiencies of human HSCs existed among the animals receiving intrahepatic, intraperitoneal and intravascular injections [28]. Another possibility is the gestational day of injection. Zanjani *et al.* [27] injected cells at days 51–71 of gestation, whereas we injected cells at days 45–49 of gestation. However, according to our previous studies [1, 2, 24, 28], the gestational day of fetal sheep for performing the cell injection (45–79 gestational days) did not affect the engraftment efficiency, either. One more possible explanation for this discrepancy is the source of cells used in the studies, as suggested by Noia *et al.* [18]. Zanjani *et al.* [31] used human fetal liver mononuclear cells, whereas we used human CB $CD34^+$ cells. Thus, it is reasonable that the transplantation of ontogenetically matched HSCs (fetal-to-fetal) results in a better outcome than that of ontogenetically mismatched HSCs (neonatal-to-fetal).

A very low level of transplant-derived cells was present (<0.01%) in the PB of the sheep, unlike in the PB of immunodeficient mice [14, 15]. This issue has been repeatedly mentioned in other studies about sheep IUT of human HSCs [1, 2, 17, 19, 20, 24, 28, 30]. A possible explanation is that the low PB chimerism is just reflected by the low BM chimerism (1–3%). Another possible explanation is xenogeneic mismatch between human HSCs and sheep stromal cells, and the mismatch may be larger than that between human HSCs and mouse stromal cells. The stromal trophic stimulations from the sheep microenvironment, such as cytokine secretion and adherent molecules, would not allow human hematopoietic differentiation, hampering human terminally differentiated cells to appear in the PB. The other possibility is attributed to innate immunity. That is the case when human HSCs were transplanted into even the most immunodeficient NOG mice. The numbers of human red blood cells (RBCs) and platelets were extremely low in PB in spite of high levels of human HSC-derived progenitors in BM [12, 13]. The poor reconstitution of human RBCs and platelets was a result of phagocytosis by macrophages [12, 13]. Though the absence of human blood cells in the PB, the fetal sheep model is suitable for long-term assessment of human HSCs. The fetal sheep model should provide a unique perspective for evaluating the engraftment and behavior of human HSCs.

Acknowledgments

We thank Yoshihiro Kitano (an ex-member in National Center for Child Health and Development, Tokyo, Japan), Satoshi Hayashi (Tokyo Mother's Clinic), Hiroaki Shibata (Tsukuba Primate Research Center, Ibaraki, Japan), Shigeo Masuda, Yujiro Tanaka, Yukiko Kishi, Yoshihisa Mizukami, Shuh-hei Fujishiro, Yutaka Furukawa, Hozumi Tanaka (Jichi Medical University, Tochigi, Japan), Suguru Nitta and Asuka Hara (Utsunomiya University) for excellent technical assistance and helpful discussions.

Support and Financial Disclosure Declaration

This study was supported partly by Japan Science and Technology Agency (JST) Yamanaka iPS Cell Special Project to Y.H., JST Center Network for Realization of Regenerative Medicine to YH, and by KAKENHI from Ministry of Education, Culture, Sports, Science and Technology of Japan to T.A., Y.H. and Y.N. The authors declare no competing financial interests.

References

1. Abe, T., Masuda, S., Ban, H., Hayashi, S., Ueda, Y., Inoue, M., Hasegawa, M., Nagao, Y., and Hanazono, Y. 2011. *Ex vivo* expansion of human HSCs with Sendai virus vector expressing HoxB4 assessed by sheep in utero transplantation. *Exp. Hematol.* 39: 47–54. [Medline] [CrossRef]
2. Abe, T., Masuda, S., Tanaka, Y., Nitta, S., Kitano, Y., Hayashi, S., Hanazono, Y., and Nagao, Y. 2012. Maternal administration of busulfan before in utero transplantation of human hematopoietic stem cells enhances engraftments in sheep. *Exp. Hematol.* 40: 436–444. [Medline] [CrossRef]
3. Aiuti, A., Slavin, S., Aker, M., Ficara, F., Deola, S., Mortellaro, A., Morecki, S., Andolfi, G., Tabucchi, A., Carlucci, F., Marinello, E., Cattaneo, F., Vai, S., Servida, P., Miniero, R., Roncarolo, M.G., and Bordignon, C. 2002. Correction of ADA-SCID by stem cell gene therapy combined with nonmyeloablative conditioning. *Science* 296: 2410–2413. [Medline] [CrossRef]
4. Antonchuk, J., Sauvageau, G., and Humphries, R.K. 2002. HOXB4-induced expansion of adult hematopoietic stem cells ex vivo. *Cell* 109: 39–45. [Medline] [CrossRef]
5. Bhatia, M., Bonnet, D., Murdoch, B., Gan, O.I., and Dick, J.E. 1998. A newly discovered class of human hematopoietic cells with SCID-repopulating activity. *Nat. Med.* 4: 1038–1045. [Medline] [CrossRef]
6. Bhatia, M., Wang, J.C., Kapp, U., Bonnet, D., and Dick, J.E. 1997. Purification of primitive human hematopoietic cells capable of repopulating immune-deficient mice. *Proc. Natl. Acad. Sci. USA* 94: 5320–5325. [Medline] [CrossRef]
7. Conneally, E., Cashman, J., Petzer, A., and Eaves, C. 1997. Expansion *in vitro* of transplantable human cord blood stem cells demonstrated using a quantitative assay of their lympho-myeloid repopulating activity in nonobese diabetic-scid/scid mice. *Proc. Natl. Acad. Sci. USA* 94: 9836–9841. [Medline] [CrossRef]
8. Doulatov, S., Notta, F., Laurenti, E., and Dick, J.E. 2012. Hematopoiesis: a human perspective. *Cell Stem Cell* 10: 120–136. [Medline] [CrossRef]
9. Higuchi, Y., Kawai, K., Yamamoto, M., Kuronuma, M., Ando, Y., Katano, I., Nakamura, M., and Suemizu, H. 2014. A novel enhanced green fluorescent protein-expressing NOG mouse for analyzing the microenvironment of xenograft tissues. *Exp. Anim.* 63: 55–62. [Medline] [CrossRef]
10. Hope, K.J., Jin, L., and Dick, J.E. 2004. Acute myeloid leukemia originates from a hierarchy of leukemic stem cell classes that differ in self-renewal capacity. *Nat. Immunol.* 5: 738–743. [Medline] [CrossRef]
11. Horn, P.A., Morris, J.C., Neff, T., and Kiem, H.P. 2004. Stem cell gene transfer—efficacy and safety in large animal studies. *Mol. Ther.* 10: 417–431. [Medline] [CrossRef]
12. Hu, Z. and Yang, Y.G. 2012. Full reconstitution of human platelets in humanized mice after macrophage depletion. *Blood* 120: 1713–1716. [Medline] [CrossRef]
13. Hu, Z., Van Rooijen, N., and Yang, Y.G. 2011. Macrophages prevent human red blood cell reconstitution in immunodeficient mice. *Blood* 118: 5938–5946. [Medline] [CrossRef]
14. Ishii, M., Matsuoka, Y., Sasaki, Y., Nakatsuka, R., Takahashi, M., Nakamoto, T., Yasuda, K., Matsui, K., Asano, H., Uemura, Y., Tsuji, T., Fukuhara, S., and Sonoda, Y. 2011. Development of a high-resolution purification method for precise functional characterization of primitive human cord blood-derived CD34-negative SCID-repopulating cells. *Exp. Hematol.* 39: 203–213, e1. [Medline] [CrossRef]
15. Ito, M., Hiramatsu, H., Kobayashi, K., Suzue, K., Kawahata, M., Hioki, K., Ueyama, Y., Koyanagi, Y., Sugamura, K., Tsuji, K., Heike, T., and Nakahata, T. 2002. NOD/SCID/gamma(c)(null) mouse: an excellent recipient mouse model for engraftment of human cells. *Blood* 100: 3175–3182. [Medline] [CrossRef]
16. Muguruma, Y., Matsushita, H., Yahata, T., Yumino, S., Tanaka, Y., Miyachi, H., Ogawa, Y., Kawada, H., Ito, M., and Ando, K. 2011. Establishment of a xenograft model of human myelodysplastic syndromes. *Haematologica* 96: 543–551. [Medline] [CrossRef]
17. Nagao, Y., Abe, T., Hasegawa, H., Tanaka, Y., Sasaki, K., Kitano, Y., Hayashi, S., and Hanazono, Y. 2009. Improved efficacy and safety of in utero cell transplantation in sheep using an ultrasound-guided method. *Cloning Stem Cells* 11: 281–285. [Medline] [CrossRef]
18. Noia, G., Ligato, M.S., Cesari, E., Visconti, D., Fortunato, G., Tintoni, M., Mappa, I., Greco, C., Caristo, M.E., Bonanno, G., Corallo, M., Minafra, L., Perillo, A., Terzano, M., Rutella, S., Leone, G., Scambia, G., Michejda, M., and Mancuso, S. 2008. Source of cell injected is a critical factors for short and long engraftment in xeno-transplantation. *Cell Prolif.* 41: 41–50. [Medline] [CrossRef]
19. Noia, G., Pierelli, L., Bonanno, G., Monego, G., Perillo, A., Rutella, S., Cavaliere, A.F., De Santis, M., Ligato, M.S., Fortunato, G., Scambia, G., Terzano, G.M., Iannace, E., Zelano, G., Michetti, F., Leone, G., and Mancuso, S. 2003. A novel route of transplantation of human cord blood stem cells in preimmune fetal sheep: the intracelomic cavity. *Stem Cells* 21: 638–646. [Medline] [CrossRef]
20. Noia, G., Pierelli, L., Bonanno, G., Monego, G., Perillo, A., Rutella, S., Cavaliere, A.F., Straface, G., Fortunato, G., Cesari, E., Scambia, G., Terzano, M., Iannace, E., Zelano, G., Michetti, F., Leone, G., and Mancuso, S. 2004. The intracoelomic route: a new approach for in utero human cord blood stem cell transplantation. *Fetal Diagn. Ther.* 19: 13–22. [Medline] [CrossRef]
21. Ott, M.G., Schmidt, M., Schwarzwaelder, K., Stein, S., Siler, U., Koehl, U., Glimm, H., Kühlcke, K., Schilz, A., Kunkel, H., Naundorf, S., Brinkmann, A., Deichmann, A., Fischer, M., Ball, C., Pilz, I., Dunbar, C., Du, Y., Jenkins, N.A., Copeland, N.G., Lüthi, U., Hassan, M., Thrasher, A.J., Hoelzer, D., von Kalle, C., Seger, R., and Grez, M. 2006. Correction of X-linked chronic granulomatous disease by gene therapy, augmented by insertional activation of MDS1-EVI1, PRDM16 or SETBP1. *Nat. Med.* 12: 401–409. [Medline] [CrossRef]
22. Piacibello, W., Sanavio, F., Severino, A., Danè, A., Gammaitoni, L., Fagioli, F., Perissinotto, E., Cavalloni, G., Kollet, O., Lapidot, T., and Aglietta, M. 1999. Engraftment in nonobese diabetic severe combined immunodeficient mice of human CD34(+) cord blood cells after *ex vivo* expansion:

evidence for the amplification and self-renewal of repopulating stem cells. *Blood* 93: 3736–3749. [Medline]
23. Peled, A., Petit, I., Kollet, O., Magid, M., Ponomaryov, T., Byk, T., Nagler, A., Ben-Hur, H., Many, A., Shultz, L., Lider, O., Alon, R., Zipori, D., and Lapidot, T. 1999. Dependence of human stem cell engraftment and repopulation of NOD/SCID mice on CXCR4. *Science* 283: 845–848. [Medline] [CrossRef]
24. Sasaki, K., Nagao, Y., Kitano, Y., Hasegawa, H., Shibata, H., Takatoku, M., Hayashi, S., Ozawa, K., and Hanazono, Y. 2005. Hematopoietic microchimerism in sheep after in utero transplantation of cultured cynomolgus embryonic stem cells. *Transplantation* 79: 32–37. [Medline] [CrossRef]
25. Sauvageau, G., Thorsteinsdottir, U., Eaves, C.J., Lawrence, H.J., Largman, C., Lansdorp, P.M., and Humphries, R.K. 1995. Overexpression of HOXB4 in hematopoietic cells causes the selective expansion of more primitive populations *in vitro* and *in vivo*. *Genes Dev.* 9: 1753–1765. [Medline] [CrossRef]
26. Schiedlmeier, B., Klump, H., Will, E., Arman-Kalcek, G., Li, Z., Wang, Z., Rimek, A., Friel, J., Baum, C., and Ostertag, W. 2003. High-level ectopic HOXB4 expression confers a profound *in vivo* competitive growth advantage on human cord blood $CD34^+$ cells, but impairs lymphomyeloid differentiation. *Blood* 101: 1759–1768. [Medline] [CrossRef]
27. Skopal-Chase, J.L., Pixley, J.S., Torabi, A., Cenariu, M.C., Bhat, A., Thain, D.S., Frederick, N.M., Groza, D.M., and Zanjani, E.D. 2009. Immune ontogeny and engraftment receptivity in the sheep fetus. *Fetal Diagn. Ther.* 25: 102–110. [Medline] [CrossRef]
28. Tanaka, Y., Masuda, S., Abe, T., Hayashi, S., Kitano, Y., Nagao, Y., and Hanazono, Y. 2010. Intravascular route is not superior to an intraperitoneal route for in utero transplantation of human hematopoietic stem cells and engraftment in sheep. *Transplantation* 90: 462–463. [Medline] [CrossRef]
29. Yahata, T., Takanashi, T., Muguruma, Y., Ibrahim, A.A., Matsuzawa, H., Uno, T., Sheng, Y., Onizuka, M., Ito, M., Kato, S., and Ando, K. 2011. Accumulation of oxidative DNA damage restricts the self-renewal capacity of human hematopoietic stem cells. *Blood* 118: 2941–2950. [Medline] [CrossRef]
30. Young, A.J., Holzgreve, W., Dudler, L., Schoeberlein, A., and Surbek, D.V. 2003. Engraftment of human cord blood-derived stem cells in preimmune ovine fetuses after ultrasound-guided in utero transplantation. *Am. J. Obstet. Gynecol.* 189: 698–701. [Medline] [CrossRef]
31. Zanjani, E.D., Flake, A.W., Rice, H., Hedrick, M., and Tavassoli, M. 1994. Long-term repopulating ability of xenogeneic transplanted human fetal liver hematopoietic stem cells in sheep. *J. Clin. Invest.* 93: 1051–1055. [Medline] [CrossRef]
32. Zhang, X.B., Beard, B.C., Beebe, K., Storer, B., Humphries, R.K., and Kiem, H.P. 2006. Differential effects of HOXB4 on nonhuman primate short- and long-term repopulating cells. *PLoS Med.* 3: e173. [Medline] [CrossRef]

OPEN ACCESS Freely available online

PLOS ONE

MHC-Matched Induced Pluripotent Stem Cells Can Attenuate Cellular and Humoral Immune Responses but Are Still Susceptible to Innate Immunity in Pigs

Yoshihisa Mizukami[1], Tomoyuki Abe[1,2], Hiroaki Shibata[3], Yukitoshi Makimura[2], Shuh-hei Fujishiro[1], Kimihide Yanase[1], Shuji Hishikawa[2], Eiji Kobayashi[2], Yutaka Hanazono[1,2,4]*

1 Division of Regenerative Medicine, Center for Molecular Medicine, Jichi Medical University, Tochigi, Japan, **2** Center for Development of Advanced Medical Technology, Jichi Medical University, Tochigi, Japan, **3** Tsukuba Primate Research Center, National Institute of Biomedical Innovation, Ibaraki, Japan, **4** CREST, Japan Science and Technology Agency, Tokyo, Japan

Abstract

Recent studies have revealed negligible immunogenicity of induced pluripotent stem (iPS) cells in syngeneic mice and in autologous monkeys. Therefore, human iPS cells would not elicit immune responses in the autologous setting. However, given that human leukocyte antigen (HLA)-matched allogeneic iPS cells would likely be used for medical applications, a more faithful model system is needed to reflect HLA-matched allogeneic settings. Here we examined whether iPS cells induce immune responses in the swine leukocyte antigen (SLA)-matched setting. iPS cells were generated from the SLA-defined C1 strain of Clawn miniature swine, which were confirmed to develop teratomas in mice, and transplanted into the testes ($n=4$) and ovary ($n=1$) of C1 pigs. No teratomas were found in pigs on 47 to 125 days after transplantation. A Mixed lymphocyte reaction revealed that T-cell responses to the transplanted MHC-matched (C1) iPS cells were significantly lower compared to allogeneic cells. The humoral immune responses were also attenuated in the C1-to-C1 setting. More importantly, even MHC-matched iPS cells were susceptible to innate immunity, NK cells and serum complement. iPS cells lacked the expression of SLA class I and sialic acids. The in vitro cytotoxic assay showed that C1 iPS cells were targeted by NK cells and serum complement of C1. In vivo, the C1 iPS cells developed larger teratomas in NK-deficient NOG (T-B-NK-) mice ($n=10$) than in NK-competent NOD/SCID (T-B-NK+) mice ($n=8$) ($p<0.01$). In addition, C1 iPS cell failed to form teratomas after incubation with the porcine complement-active serum. Taken together, MHC-matched iPS cells can attenuate cellular and humoral immune responses, but still susceptible to innate immunity in pigs.

Citation: Mizukami Y, Abe T, Shibata H, Makimura Y, Fujishiro S-h, et al. (2014) MHC-Matched Induced Pluripotent Stem Cells Can Attenuate Cellular and Humoral Immune Responses but Are Still Susceptible to Innate Immunity in Pigs. PLoS ONE 9(6): e98319. doi:10.1371/journal.pone.0098319

Editor: Vassiliki A. Boussiotis, Beth Israel Deaconess Medical Center, Harvard Medical School, United States of America

Received October 20, 2013; **Accepted** April 30, 2014; **Published** June 13, 2014

Copyright: © 2014 Mizukami et al. This is an open-access article distributed under the terms of the Creative Commons Attribution License, which permits unrestricted use, distribution, and reproduction in any medium, provided the original author and source are credited.

Funding: This study was in part supported by Japan Science and Technology Agency Research Center Network for Realization of Regenerative Medicine to YH, by KAKENHI from Ministry of Health, Labour and Welfare of Japan to YH, and by Jichi Medical University Graduate Student Start-Up Grant for Young Investigators to Y Mizukami. The funders had no role in study design, data collection and analysis, decision to publish, or preparation of the manuscript.

Competing Interests: Prof. Eiji Kobayashi is a chief scientific advisor; however, this does not alter the authors' adherence to all PLOS ONE policies on sharing data and materials.

* E-mail: hanazono@jichi.ac.jp

Introduction

Induced pluripotent stem (iPS) cells are generated from adult mature cells following transduction with the transcription factors *Oct3/4*, *Sox2*, *Klf4*, and *c-Myc* [1,2]. They have the ability to differentiate into all cell types [3,4,5] and, therefore, have considerable potential for autologous stem cell therapies [6,7]. Recently, it was shown that iPS cells do not elicit immune responses when they are transplanted into syngeneic mice [8,9] or into autologous monkeys [10,11]. Therefore, it is likely that human iPS cells would not elicit immune responses in an autologous setting [12].

However, autologous derivation of iPS cells requires considerable time and effort for their generation and for assessment of their clinical safety and efficacy. Therefore, the establishment of human leukocyte antigen (HLA)-typed banks of iPS cells for cell transplantation therapies has been proposed [13,14,15,16]. Given that such banks would involve HLA-matched allogeneic human iPS cells being used for medical applications, a better model system is needed to reflect the likely HLA-matched settings and testing and developing medical applications. As swine show close similarities in anatomy, biochemistry and physiology to humans, they have been used as a possible model system [17,18]. In addition, swine are the only large animal that have inbred MHC-defined strains available [19,20,21]. One such strain, Clawn miniature swine, was established in 1978 by Nakanishi and colleagues at Kagoshima University, and its swine leukocyte antigen (SLA) genotype was identified [20,22,23]. Previously, we established iPS cells from inbred SLA-defined Clawn miniature swine [24] (Fig. S1 in File S1). The transplantation of porcine iPS cells in an SLA-matched setting might provide a robust model for transplantation of human iPS cells in an HLA-matched setting. In the present study, we sought to determine whether iPS cells from Clawn miniature swine induce immune responses in an SLA-matched setting.

Materials and Methods

Animals

Clawn miniature swine (7- to 20-month-old male and female pigs) were purchased from Japan Farm (Kagoshima, Japan). Clawn miniature swine have two SLA haplotypes, C1 and C2 [22,23]. As shown in the genealogy (Fig. S2 in File S1), the donor animal (AT25) and the recipients (CT19, CQ38, CU65, SF65, SD57 and CQ74) were very closely related. All pigs were housed at 23–27°C under conditions of 50–70% humidity with a 12 hours light/12 hours dark cycle. All animals were housed in individual pens (1 m×1.5 m) with a bedding space (0.5 m×1 m). They were given 600 g of feed once daily.

Six-week-old non-obese diabetic/severe combined immunodeficient (NOD/SCID) and NOD/SCID/γc^{null} (NOG) male mice were purchased from CLEA Japan (Tokyo, Japan) and the Central Institute for Experimental Animals (Kawasaki, Japan), respectively. The mice were maintained under a 12 hours light/12 hours dark cycle and fed ad libitum.

All animal experiments reported here were approved by the Institutional Animal Experiment Committee of Jichi Medical University (mice 13490 and pigs 13450).

Porcine iPS cells

C1 iPS cells were established from porcine embryonic fibroblasts (PEFs) of a C1 strain animal using retroviral vectors expressing human SOX2, OCT3/4, KLF4, and c-MYC [24]. The cells were maintained on a feeder layer of mitomycin C (Kyowa-Hakko-Kogyo, Tokyo, Japan)-treated STO cells (ATCC, VA, USA) in Knockout DMEM (Invitrogen, CA, USA) supplemented with 15% fetal bovine serum (Invitrogen), 1% glutamax-L (Invitrogen), 1% nonessential amino acids (Invitrogen), 0.1 mM 2-mercaptoethanol (Invitrogen), 50 U/ml penicillin (Invitrogen), 50 μg/mL streptomycin (Invitrogen), 10 μM forskolin (Biomol International Inc), and in-house produced recombinant porcine leukemia inhibitory factor (1:200 of conditioned medium) at 38.5°C in a humidified atmosphere of 5% CO_2 in air.

Transplantation

Transplantation experiments were performed in the Center for Development of Advanced Medical Technology of Jichi Medical University and in the Japan Farm Clawn Institute. For transplantation into pigs, C1 iPS cells were harvested by trypsinization and then incubated on gelatin-coated dishes for 15 min to remove STO feeder cells. Harvested iPS cells were washed by centrifugation and suspended in 500 μL of phosphate-buffered saline (PBS). Recipient pigs were anesthetized by 5% isoflurane inhalation. The cells were injected (3×10^7 cells/site) into the testes of the C1 pigs ($n=4$) using 23-gauge needles (Terumo, Tokyo, Japan) in combination with ultrasound guidance (Fig. S2 in File S1). C1 iPS cells were also injected into the ovaries of C1 ($n=1$) and C2 ($n=1$) pigs after laparotomy (Fig. S2 in File S1). At 47 or 125 days after injection, the pigs were euthanized by administration of KCl solution under general anesthesia.

For transplantation into mice, C1 iPS cells were injected (1×10^6 cells/site) intramuscularly into the hindlimb of NOD/SCID and NOG mice using 29-gauge needles (Terumo). At 5 or 16 weeks after transplantation, the mice were euthanized and tumors were isolated.

Immunohistochemistry

Tissue samples were fixed with 4% paraformaldehyde in PBS (Wako, Osaka, Japan) and embedded in paraffin. For immunostaining, the sections were first blocked using 2% bovine serum albumin (Sigma-Aldrich, MO, USA) in PBS and then stained with anti-porcine CD3 (Abcam, MA, USA; 1:50), and anti-human CD79 (Dako, CA, USA; 1:50). Some sections were stained with hematoxylin and eosin.

Cytochemical staining

For immunocytochemistry, cells were fixed with 4% paraformaldehyde in PBS and permeabilized with 0.2% Triton X-100 in PBS (Sigma-Aldrich). The cells were then blocked with 2% bovine serum albumin in PBS and incubated with primary antibodies. The cells were washed and then incubated with fluorescence-labeled secondary antibodies and 1 μg/ml DAPI (Roche Applied Science, USA; 1:1000) to stain the nuclei. The primary antibodies used were antibodies against Oct3/4 (Santa Cruz Biotechnology, TX, USA; 1:200), SLA class I (Vmrd, WA, USA; 1:100), and CD47 (Thermo Fisher Scientific, CA, USA; 1:50). The secondary antibodies used were anti-mouse or anti-rabbit IgG conjugated with FITC (Invitrogen, 1:500) or Alexa Flour 555 (Invitrogen, 1:500).

For lectin cytochemistry, cells were incubated with biotinylated *Maackia amurensis lectin* II (MAL, Vector Laboratories, USA; 1:25) or FITC-conjugated *Sambucus nigra lectin* (SNA, Vector Laboratories, USA; 1:40) at 4°C overnight. FITC-ultravidin (Leinco Technologies, MO, USA; 1:200) was applied to the MAL-treated cells for 1 hour at room temperature.

Mixed lymphocyte reaction (MLR)

Peripheral blood mononuclear cells (PBMCs) were isolated from porcine peripheral blood using Ficoll-Paque PLUS (GE Healthcare, Buckinghamshire, UK) following the manufacturer's procedures. PBMCs from SLA-matched recipients (C1) were suspended in RPMI-1640 (Gibco) medium with 10% FBS as responder cells. Then, 1×10^5 responder cells and 2×10^4 mitomycin C-treated stimulator cells were plated in each well of 96-well U-bottomed plates (Becton Dickinson, USA) and incubated at 38.5°C for 5 days. Plates were pulsed with 1 μCi/well of ^{3}H-thymidine (GE Healthcare) for 24 hours and the cellular uptake of ^{3}H-thymidine was quantified using a β-scintillation counter (Aloka, Tokyo, Japan). Stimulation index were represented by the mean of cpm experimental/cpm unstimulated. Significant differences were examined using Student's *t*-test.

Humoral immune response

The presence of porcine IgG antibodies against C1 iPS cells in pigs was determined using a flow cytometer. C1 iPS cells were incubated with 1:10 diluted serum taken from the C1 iPS cell-transplanted C1 pigs, and from allogeneic pigs that were not C1 or C2. After secondary staining with FITC-conjugated anti-porcine IgG specific for Fc fragment (AbD Serotec, Oxford, UK), the cells were examined by FACS Calibur flow cytometer. Data acquisition and analysis were performed using CellQuest software (BD Pharmingen).

In vitro NK-cell mediated cytotoxicity assay

PBMCs were isolated by density gradient centrifugation using Ficoll-Paque PLUS to exclude polymorphonuclear cells. The cells were incubated with BD Pharm Lyse Buffer (BD Bioscience) to remove erythrocytes. The cells were labeled with a PE-conjugated anti-porcine CD16 antibody (AbD Serotec). The labeled cells were isolated with anti-PE paramagnetic microbeads (Miltenyi Biotec, Bergisch-Gladbach, Germany) according to the manufacture's instructions. The isolated cells were labeled with an FITC-conjugated anti-porcine CD3 antibody (BD Bioscience). Using a